

# Impact of bioenergy crops expansion on climate-carbon cycle feedbacks in overshoot scenarios

Irina Melnikova<sup>1,2</sup>, Olivier Boucher<sup>1</sup>, Patricia Cadule<sup>1</sup>, Katsumasa Tanaka<sup>2,3</sup>, Thomas Gasser<sup>4</sup>, Tomohiro Hajima<sup>5</sup>, Yann Quilcaille<sup>6</sup>, Hideo Shioyama<sup>3</sup>, Roland Séférian<sup>7</sup>, Kaoru Tachiiri<sup>3,5</sup>, Nicolas Vuichard<sup>2</sup>, Tokuta Yokohata<sup>3</sup> and Philippe Ciais<sup>2</sup>

<sup>1</sup>Institut Pierre-Simon Laplace (IPSL), Sorbonne Université / CNRS, Paris, France

<sup>2</sup>Laboratoire des Sciences du Climat et de l'Environnement (LSCE), IPSL, Commissariat à l'énergie atomique et aux énergies alternatives (CEA/ CNRS/ UVSQ), Université Paris-Saclay, Gif-sur-Yvette, France

<sup>3</sup>Earth System Division, National Institute for Environmental Studies (NIES), Tsukuba, Japan

<sup>4</sup>International Institute for Applied Systems Analysis (IIASA), Vienna, Austria

<sup>5</sup>Research Institute for Global Change, Japan Agency for Marine-Earth Science and Technology, Kanazawa-ku, Japan

<sup>6</sup>Institute for Atmospheric and Climate Science, ETH Zürich, Switzerland

<sup>7</sup>CNRM, Université de Toulouse, Météo-France, CNRS, Toulouse, France

Correspondence to: Irina Melnikova (irina.melnikova@lsce.ipsl.fr)

**Abstract.** Stringent mitigation pathways frame the deployment of second-generation bioenergy crops combined with Carbon Capture and Storage (CCS) to generate negative CO<sub>2</sub> emissions. This Bioenergy with CCS (BECCS) technology facilitates the achievement of the long-term temperature goal of the Paris Agreement. Here, we use five state-of-the-art Earth System models (ESMs) to explore the consequences of large-scale BECCS deployment on the climate-carbon cycle and carbon-climate feedbacks under the CMIP6 SSP5-3.4-OS overshoot scenario, keeping in mind that all these models use generic crop vegetation to simulate BECCS crops. First, we evaluate the land cover representation by ESMs and highlight the inconsistencies that emerge during translation the data from integrated assessment models (IAMs) that are used to develop the scenario. Second, we evaluate the land-use change (LUC) emissions of ESMs against bookkeeping models. Finally, we show that an extensive cropland expansion for BECCS causes ecosystem carbon loss that drives the acceleration of carbon turnover and affects the CO<sub>2</sub> fertilization effect- and climate change-driven estimates of the absolute values of the global carbon concentration  $\beta$  and carbon-climate  $\gamma$  feedback parameters and carbon uptake. Both parameters decrease so that global  $\beta$  becomes less positive, and  $\gamma$  more negative. Over the 2000–2100 period, the land-use change (land-use change (LUC) LUC) for BECCS leads to an offset of the CO<sub>2</sub> fertilization effect  $\beta$ -driven carbon uptake by 12.2% and amplifies the  $\gamma$  climate change-driven carbon loss by 14.6%. A human choice on land area allocation for energy crops should take into account not only the potential amount of the bioenergy yield but also the LUC emissions, and the associated loss of future potential change in the carbon uptake via driven by the  $\beta$  and  $\gamma$  feedbacks. The dependency of the land estimates of  $\beta$  and  $\gamma$  carbon uptake on LUC is very strong after the middle of the 21<sup>st</sup> century in the SSP5-3.4-OS scenario but it also affects other SSP scenarios and should be taken into account by the integrated assessment modelling IAM teams, and accounted for in future studies mitigation policies should further investigate the trade-offs between the carbon gains from the bioenergy yield and losses from so as to limit the reductions reduced of the  $\beta$  CO<sub>2</sub> fertilization effect CO<sub>2</sub> fertilization effect-driven carbon uptake where BECCS or land use expansion of short vegetation is applied.

Mis en forme : Indice

39 **1 Introduction**

40 All stringent future socio-economic mitigation scenarios have negative emissions that rely on carbon dioxide  
41 removal (CDR) technologies (Fuss et al., 2014, Rogelj et. al., 2018). CDR is important especially in overshoot  
42 scenarios, in which temperature temporarily exceeds the given target, e.g., the Paris Agreement temperature target,  
43 before ramping down as CO<sub>2</sub> is withdrawn artificially from the atmosphere (Jones et al., 2016a; Keller et al., 2018;  
44 Tanaka et al., 2021).

45 Bioenergy with Carbon Capture and Storage (BECCS) is one of the most cost-effective CDR technologies (Jones  
46 and Albanito, 2020; Babin et al., 2021). In BECCS, atmospheric CO<sub>2</sub> is captured ~~via photosynthesis and fixed~~  
47 ~~into plant biomass from biomass growth, and harvested~~ ~~The harvested~~ biomass is then converted into bioenergy  
48 or directly combusted and a fraction of the carbon contained in the CO<sub>2</sub> produced is recuperated and is stored in  
49 geological reservoirs without being released back to the atmosphere (Canadell and Schulze, 2014). BECCS is a  
50 nascent CDR technology that has not been proven at large spatial scales. Its potential advantages include technical  
51 feasibility and a relatively low discounted cost in future decades that allows spreading mitigation efforts over a  
52 longer period (Anderson and Peters, 2016; Dooley et al., 2018).

53 The limitations of BECCS are the requirement of potentially large land areas, a loss of biodiversity, and the need  
54 for extra water and nutrients (Heck et al., 2018; Séférian et al., 2018; Li et al., 2021). Besides, BECCS may lead  
55 to a large amount of carbon emissions from land-use change (LUC), when bioenergy crops are grown over high-  
56 carbon content ecosystems such as grassland and forest (Clair et al., 2008; Gibbs et al., 2008; Schueler et al.,  
57 2013; Smith et al., 2016; Harper et al., 2018; Whitaker et al., 2018). The LUC emissions released due to land  
58 conversion to bioenergy crops include immediate (direct) greenhouse gas (GHG) emissions as associated with the  
59 destruction of biomass and slash during LUC but also delayed (indirect) emissions from the decay of stumps and  
60 soil carbon. These emissions are termed as “carbon debt” (Clair et al., 2008; Fargione et al., 2008; Gibbs et al.,  
61 2008; Krause et al., 2018) because for BECCS to be carbon neutral, this loss of carbon must be paid back by  
62 several cycles of BECCS harvest followed by carbon geological storage, assumed to substitute with fossil carbon  
63 emissions. Using low-productivity marginal or degraded lands for the deployment of second-generation bioenergy  
64 crops (such as miscanthus or switchgrass) reduces the carbon debt because such lands have less carbon to lose.  
65 Further, soil carbon sequestration, in the long run, may even be achieved with BECCS if non-harvested residues  
66 of BECCS crops exceed the carbon input to the soil of the native ecosystems they substitute (Campbell et al.,  
67 2008; Gibbs et al., 2008; Mohr and Raman, 2013; Whitaker et al., 2018).

68 The issue with putting second-generation bioenergy crops in low-productivity lands is a need to invest large areas  
69 of land (Jones et al., 2016a; Smith et al., 2016). Currently, some land ecosystems act as a carbon sink primarily  
70 driven by the CO<sub>2</sub> fertilization effect on photosynthesis and the carbon turnover in ecosystems ~~, which is often~~  
71 ~~expressed as the carbon concentration ( $\beta$ ) feedback, although it is partly counterbalanced by the carbon-climate~~  
72 ~~( $\gamma$ ) feedback (Jones et al., 2016b; Friedlingstein et al., 2020) which expresses the loss of ecosystem carbon per~~  
73 ~~unit of global warming. The  $\beta$  and  $\gamma$  feedback parameters refer to the changes in the ecosystem carbon storage~~  
74 ~~relative to the changes in the global atmospheric CO<sub>2</sub> concentration ( $\Delta$ CO<sub>2</sub>) and global surface air temperature~~  
75 ~~(GSAT,  $\Delta$ T), respectively, relative to the pre-industrial level, so that (The changes in the carbon storage can be~~  
76 ~~decomposed into the  $\beta$  and  $\gamma$  contributions ( $\beta \times \Delta$ CO<sub>2</sub> and  $\gamma \times \Delta$ T, respectively). Here the temperature change is~~  
77 ~~taken as a proxy for the response of the ecosystem carbon storage to climate change.~~ As croplands, unlike other  
78 ecosystems, have limited potential to store additional carbon because the biomass is harvested regularly, and as

Mis en forme : Indice

79 the new croplands have a lower soil carbon stock with a short turnover time for soil carbon, the large-scale BECCS  
80 deployment must affect the land carbon ~~cycle uptake  $\beta$  and  $\gamma$  feedback parameters~~, although this has not been  
81 specifically looked at in Earth System Models (ESMs) simulation results. ~~Conventionally,  $\beta$  and  $\gamma$  are estimated  
82 at a global scale and are assumed to be responses of “natural” ecosystems to the changes in CO<sub>2</sub> and climate, so  
83 that the effects of LUC on these parameters are overlooked.~~ No study to date has estimated the effects of BECCS  
84 deployment on the terrestrial carbon cycle ~~feedback parameters~~ under ~~an~~ overshoot ~~and other~~ scenarios.  
85 In this study, we estimate the impact of large-scale BECCS deployment on the carbon ~~cycle-climate~~ feedbacks  
86 under the Shared Socioeconomic Pathway (SSP) overshoot scenario named SSP5-3.4-OS that includes mitigation  
87 policies via an increase in the land area covered by second-generation bioenergy crops for CDR (Hurtt et al.,  
88 2020). We use simulations from five Coupled Model Intercomparison Project 6 (CMIP6) ESMs to ~~decompose the  
89 global  $\beta$  and  $\gamma$  contributions to estimate LUC impacts on~~ the changes in land carbon ~~pools in ecosystems with and  
90 without LUC effects: uptake and carbon-climate feedbacks.~~

## 91 **2 Data and methods**

### 92 **2.1 SSP5-3.4-OS scenario**

93 The SSP5-3.4-OS follows the high-emission SSP5-8.5 scenario and branches from it in 2040 when aggressive  
94 mitigation policies are implemented (O’Neill et al., 2016; Meinshausen et al., 2020). The delayed mitigation leads  
95 to an overshoot of the Paris Agreement 2 °C temperature limit. In addition to a decline in fossil fuel emissions,  
96 mitigation efforts after 2040 include the expansion of second-generation bioenergy crops (for BECCS) at the cost  
97 mainly of pasture lands (Hurtt et al., 2020). There is no deforestation assumed after 2010, in order to preserve the  
98 areas with high carbon content. Second-generation bioenergy crops account for most of the new cropland areas  
99 deployed after 2040. ~~In addition, a part of the existing croplands is converted to BECCS (Figure S1).~~

### 100 **2.2 CMIP6 ESMs**

101 We use five CMIP6 ESMs that simulate the SSP5-3.4-OS (Table 1). In addition to fully coupled simulations  
102 (COU), biogeochemically (BGC) coupled simulations, where only changes in the atmospheric CO<sub>2</sub> concentration,  
103 and not the temperature, affect the carbon-cycle processes, are also provided as part of the Coupled Climate–  
104 Carbon Cycle Model Intercomparison Project (C4MIP) (Jones et al., 2016b). The combination of COU and BGC  
105 simulations allows us to study carbon ~~cycle-climate~~ feedback ~~parameters~~. ~~The BGC simulation outputs indicate  
106 the changes in the carbon fluxes driven by the CO<sub>2</sub> fertilization effect, the difference between COU and BGC  
107 simulations indicates the changes in the carbon fluxes driven by climate change.~~

108 The LUC emissions in the ESMs can be estimated as the difference in net biome production (NBP) between  
109 simulations with and without land-use change that is between the “historical” and “hist-noLu” simulations for the  
110 historical period. However, such simulation pairs for future scenarios such as SSP5-3.4-OS are not usually  
111 available. The “fLuc” (net carbon mass flux into atmosphere due to LUC) variable provided by some ESMs  
112 enables an alternative way to incompletely quantify direct LUC emissions that include <sup>2</sup>deforestation<sup>2</sup> (biomass  
113 loss during deforestation), wood harvest, and the release of CO<sub>2</sub> by harvested wood products, but exclude forest  
114 regrowth and legacy soil carbon decay or gains. Three models, IPSL-CM6A-LR, CNRM-ESM2-1, and UKESM1-  
115 0-LL under consideration, provide the variable “fLuc” (Table 1).

116 Gridded CMIP6 data, with the exception of the “fLuc” variable, were adjusted by subtracting the long-term pre-  
 117 industrial linear trend from the control (piControl) experiment at a grid level. We used the anomalies relative to  
 118 the branching year values (indicated in Table S1) for changes in carbon pools and long-term mean piControl  
 119 values for changes in carbon fluxes.

### 120 2.3 Methodology

121 ESMs do not provide necessary outputs to diagnose the specific carbon fluxes generated from the transitions to  
 122 bioenergy crops: 1) they do not treat energy crops explicitly but rather use a generic “crop” vegetation type, itself  
 123 being a grass with a higher photosynthesis rate in some models, 2) crops only cover a fraction (tile) of a model  
 124 grid box, and 3) the soil carbon pool is usually not split into tiles for each vegetation type in land surface models.

125 Hence there is no perfect way to diagnose such fluxes. We pragmatically decompose the global ~~β and γ~~  
 126 ~~contributions to the~~ changes in land carbon uptake to the contributions that are LUC- and noLUC-induced by  
 127 using three different approaches described below. ~~In all three considered approaches, the γ feedback parameter is~~  
 128 ~~estimated from BGC and COU simulations and not from radiatively coupled (RAD) simulations, where only~~  
 129 ~~changes in temperature affect the carbon cycle processes. First, RAD simulations were not available for the SSP5-~~  
 130 ~~3.4 OS pathway. Second, previous studies suggest that using COU and BGC pair for calculating feedback~~  
 131 ~~parameters may be more representative because using RAD simulations leads to nonlinearity (non-additivity) of~~  
 132 ~~β and γ feedbacks (Jones et al., 2016b; Schwinger and Tjiputra, 2018; Arora et al., 2020).~~

133 ~~We define the impacts of LUC on β and γ feedback parameters as β\*<sub>LUC</sub> and γ\*<sub>LUC</sub> (we use \* to indicate the impact~~  
 134 ~~on the feedback parameters). Previously, the LUC impacts on carbon cycle were not included into the β and γ~~  
 135 ~~feedback framework. The LUC emissions can be discussed as an anthropogenic forcing separately, from the~~  
 136 ~~feedbacks of land ecosystems to the changed CO<sub>2</sub> and climate. However, the carbon cycle cannot be absolutely~~  
 137 ~~decoupled from the land cover and LUC because the new land cover would also be influenced by the changed~~  
 138 ~~CO<sub>2</sub> and climate locally and, as a result, would affect the global β and γ values.~~

139 In the “fLuc” approach (1), we exploit the “fLuc” variable provided by most models in CMIP6. ~~We estimate the~~  
 140 ~~carbon concentration β (GtC ppm<sup>-1</sup>) and carbon climate γ (GtC °C<sup>-1</sup>) feedback parameters using BGC and COU~~  
 141 ~~simulation outputs as described in previous studies (Friedlingstein et al., 2006; Gregory et al., 2009; Jones et al.,~~  
 142 ~~2016; Melnikova et al., 2021):~~

$$143 \beta = \frac{\Delta C_{BGC}}{\Delta CO_2}, \quad (1)$$

$$144 \gamma = \frac{\Delta C_{COU} - \Delta C_{BGC}}{\Delta T}, \quad (2)$$

145 where  $\Delta C_{BGC}$  and  $\Delta C_{COU}$  indicate the changes in the land carbon pool (or cumulative uptake) in BGC and COU  
 146 simulations, respectively, and  $\Delta CO_2$  and  $\Delta T$  (from COU runs) indicate the changes in the global  $CO_2$   
 147 concentration and global mean surface air temperature (GSAT), respectively, all reported changes being relative  
 148 to pre-industrial level (piControl). Because the  $CO_2$  atmospheric concentration is not always reported in the model  
 149 output, we estimate  $\Delta CO_2$  directly from the global  $CO_2$  concentration of input4MIP data set which includes the  
 150 atmospheric  $CO_2$  concentration pathway used in the concentration-driven simulations (Meinshausen et al., 2020).  
 151 We performed the calculations using 3-year moving averages.

152 The global carbon flux, NBP that includes changes in ecosystems both with LUC and noLUC effects, cumulated  
 153 over time, approximates the changes in the land carbon pool. Thus, cumulative NBP + fLuc (because NBP and

Mis en forme : Indice

Mis en forme : Indice

Mis en forme : Indice

154 fLuc have opposite sign conventions with NBP positive sink to land) approximates the changes in the land carbon  
 155 pool of noLUC ecosystems. Thus, equations (1) and (2) may be transformed to:

156 
$$\beta = \beta_{\text{noLUC}} - \beta^*_{\text{LUC}} \tag{3}$$

157 with

158 
$$\beta_{\text{noLUC}} = \frac{f_{\text{NBP}_{\text{noLUC}}dt} + f_{\text{LUC}_{\text{noLUC}}dt}}{\Delta\text{CO}_2} \tag{4}$$

159 and

160 
$$\beta^*_{\text{LUC}} = \frac{f_{\text{LUC}_{\text{LUC}}dt}}{\Delta\text{CO}_2} \tag{5}$$

161 
$$\gamma = \gamma_{\text{noLUC}} - \gamma^*_{\text{LUC}} \tag{6}$$

162 with

163 
$$\gamma_{\text{noLUC}} = \frac{(f_{\text{NBP}_{\text{noLUC}}dt} - f_{\text{NBP}_{\text{LUC}}dt}) + (f_{\text{LUC}_{\text{noLUC}}dt} - f_{\text{LUC}_{\text{LUC}}dt})}{\Delta T} \tag{7}$$

164 and

165 
$$\gamma^*_{\text{LUC}} = \frac{f_{\text{LUC}_{\text{LUC}}dt} - f_{\text{LUC}_{\text{noLUC}}dt}}{\Delta T} \tag{8}$$

166 *In the “cropland threshold” approach (2)*, we divide the global land area into energy-crop-concentrated and no-  
 167 energy-crop (not energy-crop-concentrated) grid cells by taking into account their evolution after 2015. Hurtt et  
 168 al. (2020) reported that after 2040, cropland areas expanded “mainly due to large-scale deployment of second-  
 169 generation bioenergy crops”. We carry out a sensitivity study (Text A1) to label the given grid cell as crop-  
 170 concentrated if the cropland fraction of the grid cell is larger than a given threshold. In the sensitivity analysis, we  
 171 examine a range of post-2015 cropland fraction thresholds of the grid box area and select the [\(ESM-specific\)](#)  
 172 thresholds that best approximate the total cropland area change in 2015–2100 diagnosed by each ESM. ~~Then, we~~  
 173 ~~estimate areal  $\beta$  and  $\gamma$  by using equations (1) and (2) over the energy-crop-concentrated and no-energy-crop areas.~~  
 174 Under this approach, the treatment of LUC and noLUC lands and the attribution of the LUC effects on the carbon  
 175 ~~cycle uptake feedback parameters~~ that are relevant to BECCS are both spatially explicit. The disadvantage of this  
 176 approach is that by sampling an arbitrary fraction of crop-concentrated grid-cells, we inevitably omit some carbon  
 177 changes in cropland or encroach carbon belonging to non-crop vegetation.

178 *In the “two simulations” approach (3)*, we performed additional SSP5-3.4-OS scenario simulations by IPSL-  
 179 CM6A-LR and MIROC-ES2L. In addition to standard SSP5-3.4-OS and SSP5-3.4-OS-BGC simulations, we  
 180 performed simulations in which land use is held constant corresponding to the 1850 usage (SSP5-3.4-OS-  
 181 noLUC1850 and SSP5-3.4-OS-noLUC1850-BGC). In addition, using IPSL-CM6A-LR, we performed  
 182 simulations with 2040 land cover usage (SSP5-3.4-OS-noLUC2040 and SSP5-3.4-OS-noLUC2040-BGC). The  
 183 difference in NBP between simulations with and without LUC indicates LUC emissions, which are dominated by  
 184 bioenergy crops area expansion after 2040. ~~The  $\beta^*_{\text{LUC}}$  and  $\gamma^*_{\text{LUC}}$  are estimated as the difference in  $\beta$  and  $\gamma$~~   
 185 ~~contributions, respectively, between two sets of simulations.~~ Unlike in approaches (1) and (2), the term LUC here  
 186 incorporates a carbon source called the “loss of additional sink capacity” (LASC) relative to the reference years  
 187 1850 and 2040 (Gasser and Ciais, 2013; Pongratz et al., 2014). LASC is a change in carbon flux, or a foregone  
 188 sink, in response to environmental changes on managed land compared to potential natural vegetation. The  
 189 approach (3) accounts for the indirect LUC emissions while the approaches (1) and (2) do not.

### 190 3 Evaluation and data consistency

191 The SSP5-3.4-OS is a concentration-driven scenario based on the implementation of SSP5 in the REMIND-  
192 MAgPIE [integrated assessment model \(IAM\)](#) (Kriegler et al., 2017; Meinshausen et al., 2020). Bauer et al. (2017),  
193 Popp et al. (2017), and Riahi et al. (2017) provided [the quantifications, including additional details on the changes](#)  
194 [in energy and land use, for in the scenario by the integrated assessment model \(IAM\) scenario](#). Hurtt et al. (2020)  
195 provided the changes in land use in a coherent gridded format required for ESMs in the Harmonization of Global  
196 Land-Use Change and Management version 2 (LUH2) project. In LUH2, the historical data (up to the year 2014)  
197 based on the History of the Global Environment database (HYDE) and future scenarios (2015–2300) based on  
198 IAM are harmonized to minimize the differences between the end of historical reconstruction and IAM initial  
199 conditions (Hurtt et al., 2020). The harmonization process, however, is expected to result in some mis matches  
200 between LUH2 and the IAM during the early stage of the post-2014 period. First, we check the consistency of the  
201 global and regional cropland and other land-state areas reported by REMIND-MAgPIE, LUH2, and CMIP6  
202 ESMs. Second, we evaluate global and regional historical LUC estimates by CMIP6 ESMs against three  
203 bookkeeping approaches.

#### 204 3.1 Consistency of cropland area between REMIND-MAgPIE, LUH2, and ESMs

205 Under the SSP5-3.4-OS pathway, the cropland area increases [by  \$8.1 \times 10^6 \text{ km}^2\$  \(~50%\) from the 2010 level in the](#)  
206 [21st century to 2100 by 50% from the 2010 level in the 21st century, so that it reaches  \$8.1 \times 10^6 \text{ km}^2\$  in 2100](#)  
207 (Hurtt et al., 2020). The global cropland area modelled by REMIND-MAgPIE and downscaled by LUH2 increases  
208 due to the expansion of second-generation bioenergy crops. The global cropland areas by REMIND-MAgPIE and  
209 LUH2 are largely consistent with a slightly larger area of crops by REMIND-MAgPIE till the 2050s (reaching  
210  $0.6 \times 10^6 \text{ km}^2$  in the year 2050) and a larger area of crops by LUH2 in 2060 – 2090s (Figure [S21a](#)). Unlike the  
211 REMIND-MAgPIE, LUH2 simulates a slight reduction of forest area (by  $1.3 \times 10^6 \text{ km}^2$  in 2100 from 2010 level).  
212 [The global cropland area in LUH2 is less than in REMIND-MAgPIE by  \$0.3 \times 10^6 \text{ km}^2\$  in 2015, and larger by  \$2.9\$](#)   
213  [\$\times 10^6 \text{ km}^2\$  in 2060. The differences in the global cropland area between LUH2 and REMIND-MAgPIE reach  \$2.9\$](#)   
214  [\$\times 10^6 \text{ km}^2\$  in the year 2060](#) that is 14% of the total cropland area of  $20.7 \times 10^6 \text{ km}^2$  by LUH2 in 2060 (and  
215 corresponds to a 43.4% increase from the 2015 level) and may cause additional uncertainty in estimates of the  
216 BECCS area and LUC. Further, ESMs implement the global and regional gridded cropland fractions following  
217 LUH2 and using their own land cover map (Figure [S21b](#)), with an exception of UKESM1-0-LL that reports an  
218 evolution of the global cropland area smaller than those of other ESMs. This deviation of UKESM1-0-LL may  
219 occur because of its specifications in the treatment of croplands and the model's dry bias (precipitation deficit) in  
220 India and the Sahel (Sellar et al., 2019). While the model uses the LUH2 data to prescribe an area available for  
221 crops to grow in, this area is covered by the crop PFTs only if the model's climate is suitable for the grass PFTs,  
222 otherwise, the area remains bare soil.

223 Aside from the deviations in total areas of land cover types between REMIND-MAgPIE, LUH2, and ESMs listed  
224 above, a discrepancy arises from the implementation of LUH2's land cover types to the ESM's plant functional  
225 types (PFTs). Nevertheless, most CMIP6 ESMs produce croplands area consistent with LUH2. However, the other  
226 vegetation classes of LUH2 (e.g., forested lands, non-forested lands, pastures) do not match the PFTs of ESMs  
227 because most ESMs decided to use their own land cover map rather than used the LUH2 one for these ecosystems.  
228 First, spatial distributions of vegetation classes are tightly associated with climate and biogeochemical processes,

Mis en forme : Allemand (Autriche)

Mis en forme : Allemand (Autriche)

Mis en forme : Allemand (Autriche)

Mis en forme : Allemand (Autriche)

229 and thus, the replacement of the vegetation covers in ESMs would lead to large changes in the model  
230 performances. Second, some models that include dynamic vegetation, like UKESM1-0-LL, predict the vegetation  
231 distribution change, and sometimes the predicted distribution does not coincide with the [one real one prescribed](#)  
232 [by LUH2](#). Besides, the pastures of REMIND-MAGPIE are translated to two land-use states in LUH2: pastures,  
233 and rangelands. While they are treated predominantly as low-productivity areas in REMIND-MAGPIE, this may  
234 not be a case in ESMs, where pastures and rangelands may correspond to grasslands and perhaps to shrublands  
235 (if this land cover exists in an ESM). [Some ESMs do not distinguish treat pastures and rangelands at all because](#)  
236 [of the ambiguity in their definitions. Likewise, the SSP5-3.4-OS scenario involves a large-scale second-generation](#)  
237 [bioenergy crops whose benefit is the capability to grow in so-called “marginal” lands \(Krause et al., 2018\). The](#)  
238 [ambiguity and inconsistency in the definition of land-use and land-cover tiles between IAM, LUH2 and ESMs](#)  
239 [may have implications to the interpretation of the scenario.](#)

240 We shed light on an issue of inconsistency when translating LUC from IAMs into LUH2 and, then, into ESMs.  
241 Overall, implementation of the LUC scenario of REMIND-MAGPIE to first, LUH2, and then ESMs leads to a  
242 consistency loss of simulated scenario [during the harmonization process. Further, the land cover representation](#)  
243 [in ESMs is subjective and different from the IAM and LUH2 mainly because of ambiguity in the correspondence](#)  
244 [between land-use and land-cover tiles vegetation type definitions.](#) This problem requires thorough attention ~~in a~~  
245 [separate study especially in ESMs and IAMs intercomparison studies.](#)

### 246 3.2 Evaluation of land-use change emissions

247 The global and regional LUC emissions estimated by ESMs were evaluated against three bookkeeping models for  
248 the historical period, namely BLUE (Hansis et al., 2015), HN2017 (Houghton and Nassikas, 2017), and OSCAR  
249 (Gasser et al., 2020). The models differ in the spatial units (spatially explicit, country level, region level),  
250 parametrization, and process representations (Friedlingstein et al., 2020; Gasser et al., 2020). Unlike other  
251 bookkeeping models, OSCAR also reported LASC in LUC estimates but the utilized version did not include peat  
252 emissions.

253 Unlike the difference in NBP between simulations with and without LUC, the “fLuc” variable accounts only for  
254 the direct LUC emissions and does not account for all the fluxes reported by bookkeeping models, e.g., forest  
255 regrowth and slash and soil organic matter decay, as well as for shifting cultivation and degradation (Houghton  
256 and Nassikas, 2017). Thus, its values are expected to be lower. We use an average of multiple realizations when  
257 provided by the model teams (details in Table S1). The evaluation targets estimating LUC emissions in “fLuc”  
258 and “two simulations” approaches.

259 We found that ESMs tend to estimate lower global LUC emissions than bookkeeping models by both “fLuc”  
260 variable and “two simulations” approaches (Figure 42). This is remarkable in the three tropical regions that  
261 dominate global LUC emissions since the 1960s, and particularly South and Southeast Asia (Figure S13). In 1960–  
262 2014, on average, bookkeeping models estimate that three tropical regions account for  $56.8 \pm 2.3\%$  of global LUC  
263 emissions, while ESMs estimate that they account for  $35 \pm 10\%$  based on simulations with and without LUC and  
264  $40 \pm 15\%$  based on the “fLUC” variable.

265 LUC emission estimates by MIROC-ES2L (for which only LUC emissions derived from simulations with and  
266 without LUC were available) are the most consistent with the estimates of bookkeeping models among considered  
267 ESMs (see also Liddicoat et al (2021)). We excluded the estimates of LUC emissions by CNRM-ESM2-1 based

268 on simulations with and without LUC and by UKESM1-0-LL based on “fLuc” from the analysis. CNRM-ESM2-  
269 1 estimates much lower LUC emissions derived from simulations with and without LUC than other ESMS possibly  
270 because the CMIP6 version of the model does not include a harvest module, i.e., croplands are modelled as natural  
271 grasslands (Séférián et al., 2019), and cropland soils continue to be loaded by harvest inputs. UKESM1-0-LL  
272 estimates implausibly low LUC emissions derived from the “fLuc” variable.

273 The LUC emissions estimated by the two approaches differ remarkably due to inconsistent “fLuc” definitions  
274 among models (Gasser and Ciais, 2013). We call for a clearer and more rigorous definition of this variable in  
275 future MIPs so that model outputs can be compared on the same basis. As some examples for improvement, we  
276 suggest that model teams provide [explicit detail of processes that contribute to variables contained within](#) “fLuc”,  
277 e.g., direct deforestation and wood harvest emissions, decomposition flux, as well as indirect emissions, e.g., per  
278 each PFT.

### 279 **3.3 Evaluation of land-use change emissions from BECCS deployment**

280 [The increased LUC emissions to account for BECCS are a part of total carbon budget calculations in the IAM](#)  
281 [scenario. We compared LUC emissions by different approaches using ESMS with LUC of REMIND-MAgPIE](#)  
282 [\(Figure S2\). While the IAMs design the scenario in a way that the benefits of BECCS exceed the carbon losses](#)  
283 [from LUC, the ability of IAM to accurately estimate LUC emissions including legacy emissions, LASC and long-](#)  
284 [term consequences is questionable/doubtful. Particularly in SSP5-3.4-OS scenario, the REMIND-MAgPIE](#)  
285 [estimates lower LUC emission compared ESMS.](#)

286 BECCS dominates negative emissions in the SSP5-3.4-OS pathway. We confirmed that BECCS is predominantly  
287 deployed in low-carbon uptake areas by comparing the changes in carbon pools and NBP globally and crop-  
288 concentrated areas (Figure S3S4). Because bioenergy crops are deployed in low-carbon uptake areas and they  
289 dominate LUC emissions in the 21st century, the NBP over crop-concentrated areas derived by the “cropland  
290 threshold” approach approximates global LUC emissions (Figure S5). The comparison of NBP in crop-  
291 concentrated grids with the original LUC emissions of the REMIND-MAgPIE IAM scenario confirms a similar  
292 trend between IAM-based global LUC emissions and ESMS-based global temporal NBP changes in the crop-  
293 concentrated areas after 2040. The strong correlation is evident in three ESMS, namely CanESM5, UKESM1-0-  
294 LL, and MIROC-ES2L (correlation coefficient is 0.72 for the 2015–2100 period). The carbon loss in the crop-  
295 concentrated areas over the 21<sup>st</sup> century period averaged over these three ESMS reaches  $37.8 \pm 30.3$  GtC. Two  
296 models, IPSL-CM6A-LR and CNRM-ESM2-1, however, do not capture the increased carbon loss after 2040  
297 perhaps due to low estimates of LUC emissions from crop expansion (especially, CNRM-ESM2-1) or  
298 overestimated uptake by no-LUC areas (Figures 42, S13). Besides, IPSL-CM6A-LR simulates the lowest  
299 ecosystem carbon pool, especially in soils (Arora et al., 2020, Figure S46) that may lead to relatively small LUC-  
300 induced carbon losses when cropland areas expand. Thus, the estimates of LUC impact on carbon ~~cycle~~-climate  
301 feedbacks from IPSL-CM6A-LR and CNRM-ESM2-1 need to be considered with the above-mentioned caveats.



## 4 The impact of LUC ~~from bioenergy crops expansion~~ on the carbon ~~cycle uptake feedback parameters~~

### 4.1 Differences in LUC impact on carbon ~~cycle uptake~~ estimated by three approaches

We use the estimates of the LUC impacts on global  ~~$\beta$  and  $\gamma$  carbon uptake~~ by IPSL-CM6A-LR and MIROC-ES2L to compare the three approaches described in section 2.3 between each other. ~~The estimates of both models and three approaches show that the LUC impacts lead to a loss of carbon fluxes (Figure 3). The losses from LUC surpass the benefits from the CO<sub>2</sub> fertilization effect, so that the LUC ecosystems become a carbon source to the atmosphere. The differences arise from the peculiarities of each approach.~~ The “cropland threshold”, unlike the other two approaches, separates cropland-concentrated and no-crop contributions spatially. Thus, the estimated ~~changes in carbon cycle feedback parameters uptake~~ are areal cumulative ~~under the “cropland threshold” approach~~. In the other two approaches, in contrast, the  ~~$\beta$  and  $\gamma$  changes in carbon fluxes~~ are calculated in each grid cell for both LUC-dominated and noLUC ecosystems, so that carbon change of these two land-use categories may partly offset each other. ~~For this reason, the carbon cycle feedback parameters, especially  $\beta$ , estimated via “cropland threshold” are of smaller magnitudes (sometimes by several times) than those estimated via the “two simulations since 1850” approach (Figure 2).~~

A larger loss is seen in “two simulations since 1850” because these simulations include LASC and legacy soil emissions (Figure 2a3a). Intermediate loss is from “fLUC” because this approach includes only immediate (direct) carbon loss. Lower carbon losses correspond to “cropland threshold” approach that also includes a carbon sink in natural ecosystems over selected grid cells and misses initial carbon loss, and to “two simulations since 2040” that misses legacy emissions of activities before 2040. The larger carbon losses in the “two simulations since 1850” than in the “two simulations since 2040” estimates also reveal the long-term effects of LUC.

In the case of IPSL-CM6A-LR, ~~the “fLUC” and “two simulations” approaches suggest that a BECCS related carbon loss leads to a negative  $\beta_{LUC}^*$ , and the “cropland threshold” and “two simulations” approaches suggest that a carbon loss and climate effects on enhancing soil carbon decomposition leads to a negative  $\gamma_{LUC}^*$ .~~ The “cropland threshold” and “two simulations since 2040” approaches produce similar estimates of LUC impact on cumulative  ~~$\beta$  and  $\gamma$  contributions to land carbon uptake~~ because these two methods target the changes in the carbon fluxes particularly due to cropland expansion for BECCS in the 21<sup>st</sup> century (Figure 2). MIROC-ES2L that accounts for gross LUC emissions (Liddicoat et al., 2021) produces similar estimates of LUC impact by “cropland threshold” and “two simulations since 1850” approaches ~~(except for differences in  $\beta$  explained above)~~.

### 4.2 Temporal impacts of LUC on global ~~$\beta$ and $\gamma$ carbon uptake~~

Figure 43 illustrates the attribution of global  ~~$\beta$  and  $\gamma$  driven~~ carbon fluxes to LUC- (or crop-concentrated) and no-LUC (no-crop) ecosystems by five ESMs and three approaches ~~(see Figure S4 for the results, specific for each ESM and approach)~~. The large-scale deployment of bioenergy crops even on low carbon-uptake areas causes a carbon loss from the ecosystem. ~~The negative values of the carbon flux in the CO<sub>2</sub> concentration only simulation indicate the domination of the LUC losses over the CO<sub>2</sub> fertilization effect-driven carbon gains in the ecosystems.~~ For the “cropland threshold” approach, the majority of ESM simulations, excluding IPSL-CM6A-LR and CNRM-ESM2-1 (see section 3.3), agree that cropland expansion causes a decrease in global ~~CO<sub>2</sub> fertilization effect-driven carbon uptake  $\beta$ , especially and that  $\beta$  is negative~~ in crop-concentrated grids which lose carbon from LUC ~~(Figure 3, Table S2)~~. Cropland expansion for BECCS may also contribute to the global ~~climate change-driven change towards more negative values (larger carbon source) loss~~. However, these changes are small in the “cropland

341 threshold” and absent in “fLUC” estimates. We speculate this occurs because the “fLuc” variable involves only  
342 direct LUC changes such as deforestation, wood harvest, and soil carbon decay. On top of it, earlier findings show  
343 that the ESMs ~~misrepresent do not realistically represent~~ the ~~amplitude and ratedynamics~~ of ~~changes in~~ soil and  
344 litter carbon after LUC (Brovkin-Boysen et al., 2021).

345 ~~The  $\gamma$  estimates are in less agreement between ESMs than  $\beta$ , and they are more uncertain when estimated from~~  
346 ~~BGC and COU simulations, as opposed to RAD runs (Schwinger and Tjiputra, 2018).~~ The LUC carbon losses for  
347 BECCS deployment cannot be overridden by the increased CO<sub>2</sub> effects (Figure S7) ~~but they. This causes a~~  
348 ~~decrease in the global  $\beta$  feedback parameter. Although more studies are needed to confirm t~~ ~~The impacts of~~  
349 ~~BECCS associated LUC carbon losses on the global  $\gamma$ , the majority of simulations confirm a contribution of LUC~~  
350 ~~ecosystems contribute~~ to the ~~negative  $\gamma$  carbon losses driven by the climate change~~. Overall, the three approaches  
351 and five ESMs demonstrate that the BECCS expansion under the SSP5-3.4-OS pathway results in  $42.55 \pm 41.08$   
352 GtC loss that corresponds to 12.2% of noLUC ~~CO<sub>2</sub> fertilization~~ $\beta$ -driven uptake and to an additional  $13.00 \pm 12.27$   
353 GtC loss that corresponds to 14.6% of noLUC  ~~$\gamma$  climate change~~-driven loss over the 2000–2100 period (Tables S2  
354 ~~and S3~~).

#### 355 4.3 Spatial variation of impacts of LUC on global ~~$\beta$ and $\gamma$~~ carbon uptake

356 ~~The~~ We investigated the spatial variation of ~~LUC impact on  $\beta$  and  $\gamma$~~  the land carbon cycle ~~differs among using~~  
357 ~~simulations with and without LUC by MIROC-ES2L and IPSL-CM6A-IR ESMs but the majority agrees on the~~  
358 ~~globally positive  $\beta$  with larger magnitude in the low latitudes and on the positive and negative  $\gamma$  in the northern~~  
359 ~~high latitudes and low latitudes, respectively (Figure S 54, S8).~~

360 ~~The ESMs agree on the globally positive  $\beta$  with larger magnitude in the low latitudes and on the positive and~~  
361 ~~negative  $\gamma$  in the northern high latitudes and low latitudes, respectively.~~

362 ~~Two models~~ The carbon cycle feedback parameters are expected to increase after the peak of CO<sub>2</sub> concentration  
363 and temperature. Melnikova et al. (2021) reported that in the SSP5-3.4-OS scenario, the global  $\beta$  and  $\gamma$  parameters  
364 continue to increase even after the peaks of CO<sub>2</sub> concentration and temperature at least till the end of the 21<sup>st</sup>  
365 century due to the inertia of the Earth system. ~~After the start of BECCS deployment, t~~ ~~In 2090-2100, show that t~~  
366 ~~the  $\beta$  parameter carbon uptake is decreases~~ ~~increases~~ globally except for in the BECCS areas ~~due to LUC~~  
367 ~~emissions, especially in the tropical region, where it becomes negative (Figure 4). These differences are apparent~~  
368 ~~in CanESM5, UKESM1-0 LL, and MIROC-ES2L. The two models agree and to a lesser scale on the increase in~~  
369 ~~negative  $\gamma$  over BECCS areas due to LUC, although the simulation results of MIROC-ES2L suggest a decrease~~  
370 ~~of  $\gamma$  towards less negative in some areas of bioenergy crops deployment. positive  $\gamma$  parameter increases in the high~~  
371 ~~latitudes except for the areas of the eastern part of North America and part of Europe almost exactly in the areas~~  
372 ~~of BECCS deployment, where the  $\gamma$  is zero or negative (Figure S8). The increase in negative  $\gamma$  over low latitudes~~  
373 ~~occurs both in the areas with and without the presence of BECCS. E~~ Even though the SSP5-3.4-OS scenario is  
374 designed so that BECCS utilizes low carbon areas to cause the least possible impact on the carbon sink in  
375 unmanaged lands, these BECCS areas lose their  ~~$\beta$  CO<sub>2</sub> fertilization~~-driven carbon uptake potential but do not  
376 escape ~~climate change~~ $\gamma$ -driven carbon losses. ~~In the SSP5-3.4-OS scenario, second-generation biofuel cropland~~  
377 ~~areas estimated by LUH2 reach nearly 6% of global land (potentially vegetated) area in 2100. Assigning such vast~~  
378 ~~areas to bioenergy crops – even if they correspond to low-carbon content ecosystems – affects the land carbon~~  
379 ~~uptake and the global carbon cycle feedbacks. The decision on the assignment of these areas for energy crops~~

Mis en forme : Indice

380 requires assessment of both the current state of the ecosystem, e.g., the carbon content in vegetation and soil, and  
381 the future potential increase in the carbon uptake. The impact of LUC on the carbon cycle should be accounted  
382 for in developing future mitigation pathways so that the benefits of BECCS are not minimized by the carbon  
383 losses.

### 384 **5 The carbon cycle feedback framework perspective**

385 The CO<sub>2</sub> fertilization effect- and climate change-driven changes in the carbon fluxes and storages may be  
386 expressed as  $\beta$  and  $\gamma$  feedback parameters per unit changes in the global atmospheric CO<sub>2</sub> concentration ( $\Delta\text{CO}_2$ )  
387 and surface air temperature ( $\Delta T$ ), respectively (Jones et al., 2016b; Friedlingsstein et al., 2020; Zhang et al., 2021).  
388 Here the temperature change is taken as a proxy for the response of the ecosystem carbon storage to climate  
389 change. The spatial variation of  $\beta$  and  $\gamma$  in simulation with and without LUC by MIROC-ES2L and IPSL-CM6A-  
390 LR also demonstrates a decrease in positive  $\beta$  and to a lesser scale an increase in negative  $\gamma$  over BECCS areas  
391 (Figure S9). The carbon-concentration  $\beta$  (GtC ppm<sup>-1</sup>) and carbon-climate  $\gamma$  (GtC °C<sup>-1</sup>) feedback parameters can  
392 be estimated using BGC and COU simulation outputs (Friedlingsstein et al., 2006; Gregory et al., 2009; Jones et  
393 al., 2016; Melnikova et al., 2021; Zhang et al., 2021):

$$394 \beta = \frac{\Delta C_{\text{BGC}}}{\Delta \text{CO}_2} \quad (1)$$

$$395 \gamma = \frac{\Delta C_{\text{COU}} - \Delta C_{\text{BGC}}}{\Delta T} \quad (2)$$

396 where  $\Delta C_{\text{BGC}}$  and  $\Delta C_{\text{COU}}$  indicate the changes in the land carbon pool (or cumulative uptake) in BGC and COU  
397 simulations, respectively, and  $\Delta \text{CO}_2$  and  $\Delta T$  (from COU runs) indicate the changes in the global CO<sub>2</sub>  
398 concentration and mean surface air temperature, respectively, all reported changes being relative to pre-industrial  
399 level (piControl).

400 The  $\beta$  and  $\gamma$  carbon cycle feedback framework is often compared between ESMs in idealized scenarios (such as  
401 1% CO<sub>2</sub> increase), and the  $\beta$  and  $\gamma$  feedback parameters / metrics are ~~parameters are assumed to be a pure response~~  
402 ~~to the CO<sub>2</sub> concentration and temperature changes.~~ Applying this framework to non-idealized and more socially  
403 relevant scenarios provides another perspective for understanding the changes in the carbon fluxes under more  
404 realistic evolutions. Previously, Melnikova et al. (2021) applied the  $\beta$  and  $\gamma$  framework to the SSP5-3.4-OS  
405 scenario and showed an amplification of the feedback parameters after the CO<sub>2</sub> concentration and temperature  
406 peaks due to inertia of the Earth system. Here we performed an estimation of the  $\beta$  and  $\gamma$  feedback parameters to  
407 investigate the impacts of the LUC on the behavior of the feedback parameters.

408 Note, in the case of the overshoot scenarios, if the CO<sub>2</sub> concentration and temperature changes during the ramp-  
409 down period went to zero, the definitions described in the equation 1 and 2 would become invalid. Although  
410 because in this study the change in CO<sub>2</sub> concentration and temperature never goes to zero (in the SSP5-3.4-OS  
411 before 2300), and the feedbacks parameters can safely be calculated, the limitation should be taken into account.  
412 The land carbon uptake and the  $\beta$  and  $\gamma$  feedback parameters are affected by LUC, so that they are lower in the  
413 simulations with LUC (Figure 6). Moreover, the difference in the  $\beta$  parameter estimated by IPSL-CM6A-LR in  
414 simulations with LUC and without LUC after year 2040 suggests that even only LUC for bioenergy crops  
415 expansion affects the hysteresis behaviour of the carbon cycle feedback parameters under declining CO<sub>2</sub>  
416 concentration and temperature.

417 To date, the LUC impacts on carbon cycle have not been included into the  $\beta$  and  $\gamma$  feedback framework, and the  
418 LUC emissions are discussed as an anthropogenic forcing separately from the feedbacks of land ecosystems to  
419 the changed CO<sub>2</sub> and climate. However, the  $\beta$  and  $\gamma$  parameters cannot be decoupled either from the state of the  
420 land use, or from the pre-industrial state of land cover, or from other model structural parts, leading to a value for  
421 equilibrium carbon stock. There is an interplay between land cover and the model's response to CO<sub>2</sub> (and climate)  
422 that has been demonstrated mathematically in Gasser & Ciais (2013) and defined as LASC. Gasser et al. (2020)  
423 quantified it to be a foregone sink of about 30 GtC over the historical period. But this value can only increase as  
424 future CO<sub>2</sub> will be much higher than in the past.

425 However, they are also a function of the land cover. In the SSP5 3.4 OS scenario, second generation biofuel  
426 cropland areas estimated by LUH2 reach nearly 6% of global land (potentially vegetated) area in 2100. Assigning  
427 such vast areas to bioenergy crops – even if they correspond to low carbon content ecosystems – affects the land  
428 carbon uptake and the global carbon cycle feedback parameters. The decision on the assignment of these areas for  
429 energy crops requires assessment of both the current state of the ecosystem, e.g., the carbon content in vegetation  
430 and soil, and the future potential increase in the carbon uptake via the  $\beta$  and  $\gamma$  feedbacks. The dependency of  
431 global  $\beta$  and  $\gamma$  on LUC should be accounted for in developing future mitigation pathways so that the benefits of  
432 BECCS are not minimized by adverse modulations of carbon cycle feedback parameters.

433 In a broader sense, the land-cover and land-use associated differences in the initial conditions of ESMs simulations  
434 influence the estimates of global carbon cycle feedback parameters even under idealized pathways. The  
435 divergences in the pre-industrial land covers among ESMs lead to spatial differences in the ecosystem carbon  
436 stocks (e.g., ESM with larger forest cover has larger land carbon pool size). Furthermore, the pre-industrial levels  
437 of ecosystem carbon stock vary among models even for identical land-cover types. The estimated global  $\beta$  and  $\gamma$   
438 feedback parameters involve these land-cover-related uncertainties. Future studies should address the issue by  
439 benchmarking the sets of idealized experiments with different types of land-cover and land-use changes.

440  
441 We explored the drivers of the  $\beta$  and  $\gamma$  driven carbon losses by analysing the changes in the spatial distribution  
442 of ecosystem carbon turnover time  $\tau_{\text{eco}}$ , defined as the ratio of land carbon stock to net primary production (NPP).  
443 Previous studies demonstrated that land-use change is a major driver of  $\tau_{\text{eco}}$  decrease (Wu et al., 2020; Erb et al.,  
444 2016). We found that the majority of ESMs (with an exception of CNRM-ESM2-1) show an acceleration of carbon  
445 turnover in the areas of BECCS deployment due to LUC driven ecosystem carbon loss (Figure S10 S55a-c). The  
446 carbon cycle feedback parameters are directly correlated with  $\tau_{\text{eco}}$  over the areas of BECCS deployment, which is  
447 apparent in CanESM5, UKESM1-0-LL, and MIROC-ES2L (Figure S10 d, e). LUC causes an ecosystem carbon  
448 loss that drives the acceleration of carbon turnover and results in alteration of  $\beta$  and  $\gamma$  feedback parameters.

449 The  $\beta$  and  $\gamma$  feedback parameters are assumed to be a pure response to the CO<sub>2</sub> concentration and temperature  
450 changes. However, they are also a function of the land cover. In the SSP5 3.4 OS scenario, second generation  
451 biofuel cropland areas estimated by LUH2 reach nearly 6% of global land (potentially vegetated) area in 2100.  
452 Assigning such vast areas to bioenergy crops – even if they correspond to low carbon content ecosystems – affects  
453 the land carbon uptake and the global carbon cycle feedback parameter. The decision on the assignment of these  
454 areas for energy crops requires assessment of both the current state of the ecosystem, e.g., the carbon content in  
455 vegetation and soil, and the future potential increase in the carbon uptake via the  $\beta$  and  $\gamma$  feedbacks. The

456 ~~dependency of global  $\beta$  and  $\gamma$  on LUC should be accounted for in developing future mitigation pathways so that~~  
457 ~~the benefits of BECCS are not minimized by adverse modulations of carbon cycle feedback parameters.~~

## 458 **5.6 Conclusion**

459 In this study, we investigated the impacts of bioenergy crop deployment on the ~~carbon concentration  $\beta$  and carbon-~~  
460 ~~climate  $\gamma$  feedback parameters~~ carbon cycle under an overshoot pathway. ~~In a broader sense, the land cover and~~  
461 ~~land use associated differences in the initial conditions of ESMs simulations may influence the estimates of global~~  
462 ~~carbon cycle feedback parameters even under the idealized pathways. The divergences in the pre-industrial land~~  
463 ~~covers among ESMs lead to spatial differences in the ecosystem carbon stocks (e.g., ESM with larger forest cover~~  
464 ~~has larger land carbon pool size). Furthermore, the pre-industrial levels of ecosystem carbon stock vary among~~  
465 ~~models even for identical land cover types. The estimated global  $\beta$  and  $\gamma$  feedbacks compromise involve these~~  
466 ~~land cover related uncertainties. While the  $\beta$  and  $\gamma$  are often compared between ESMs in idealized scenarios (such~~  
467 ~~as 1% CO<sub>2</sub> increase), the land cover impacts have not been discussed. Future studies should address the issue by~~  
468 ~~benchmarking the sets of idealized experiments with different types of land cover and land use changes.~~

469 In the evaluation part of this study, we highlighted some inconsistencies in the land-use states and their temporal  
470 transitions between the REMIND-MAGPIE, LUH2, and ESMs. ~~While These differences in LUC may arise from~~  
471 ~~differences in process representations~~ and initial conditions, as well as land-use and land-cover tiles definitions  
472 ~~across models and initial conditions,~~ we emphasize that ~~t~~ The inconsistencies should be taken into account in  
473 comparative studies of IAMs and ESMs. Further work will be required to address the issue of the level of  
474 inconsistency between the IAMs, LUH2, and ESMs that should be tolerated to have confidence that ESMs and  
475 IAMs describe the same scenario.

476 We exploit five ESMs and three approaches to show that cropland expansion for BECCS causes a carbon loss  
477 even in low-carbon uptake lands and reduces the future potential increase in the global carbon uptake via LUC  
478 impact on the carbon stock, and the carbon-concentration and carbon-climate feedbacks. Under the SSP5-3.4-OS,  
479 the LUC emissions from BECCS deployment cause a decrease in global  $\beta$ CO<sub>2</sub> fertilization effect-driven carbon  
480 uptake and contribute to increase the negative  $\gamma$  climate change-driven feedback parameter ~~carbon loss. The fact~~  
481 ~~that the impact on  $\beta$  dominates that on  $\gamma$ , which probably reflects the larger role of  $\beta$  driven carbon uptake than~~  
482 ~~that of  $\gamma$  driven loss in the current world and under overshoot pathways (of moderate level).~~

483 Our results are consistent with the IPCC special report on climate change and land (Shukla et al., 2019) and  
484 highlight the need for considering trade-offs in BECCS deployment and other land-uses but, to some extent, they  
485 go beyond this assessment by considering the implication of carbon cycle feedbacks. Our work shows that areas  
486 best suited for BECCS should also be assessed both in terms of their potential amount of the bioenergy yield and  
487 potential future impact on the  $\beta$  and  $\gamma$  carbon-climate feedback parameters. Future studies need to further  
488 investigate the potential of BECCS to provide negative carbon emissions with little loss of storage from the  $\beta$  and  
489  $\gamma$  feedbacks LUC. We define the impacts of LUC on  $\beta$  and  $\gamma$  feedback parameters as  $\beta^*_{LUC}$  and  $\gamma^*_{LUC}$  (we use \* to  
490 indicate the impact on the feedback parameters). Previously, the LUC impacts on carbon cycle were not included  
491 into the  $\beta$  and  $\gamma$  feedback framework. The LUC emissions can be discussed as an anthropogenic forcing separately  
492 from the feedbacks of land ecosystems to the changed CO<sub>2</sub> and climate. However, the carbon cycle cannot be  
493 absolutely decoupled from the land cover and LUC because the new land cover would also be influenced by the  
494 changed CO<sub>2</sub> and climate locally and, as a result, would affect the global  $\beta$  and  $\gamma$  values.

Mis en forme : Indice

495

496 **Data availability**

497 The data from the CMIP6 simulations are available from the CMIP6 archive ([https://esgf-](https://esgf-node.llnl.gov/search/cmip6)  
498 [node.llnl.gov/search/cmip6](https://esgf-node.llnl.gov/search/cmip6)), the LUH2 data from <https://luh.umd.edu/data.shtml>, and the IIASA database via  
499 <https://tntcat.iasa.ac.at/SspDb/dsd?Action=htmlpage&page=welcome>. We obtained LUC emission data of  
500 bookkeeping approaches from the modelling teams and <https://dare.iasa.ac.at/103/> for OSCAR.

501 **Author Contributions**

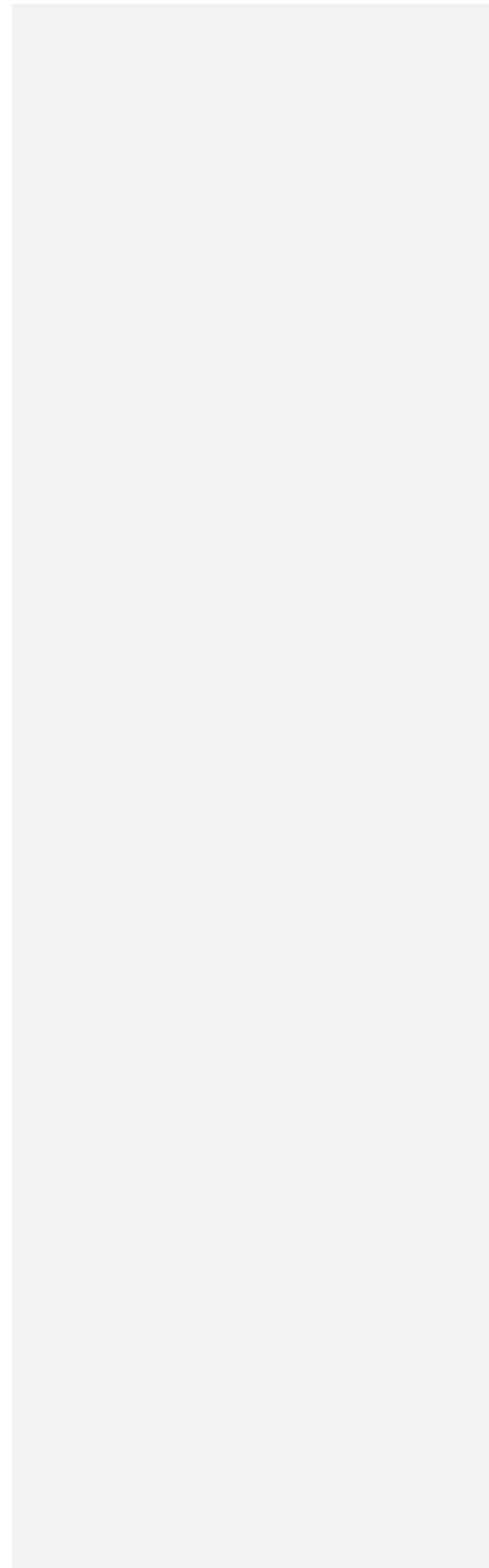
502 O.B., P.Ciais, K.Tanaka, and I.M. initiated the study, all co-authors provided input into developing the study  
503 ideas. I.M. performed data analysis and wrote the initial draft. T.H. (MIROC-ES2L) and P.Cadule (IPSL-CM6A-  
504 LR) performed additional ESM simulations. All authors contributed to writing and commenting on the paper.

505 **Competing Interests**

506 The authors have the following competing interests: Roland Séférian is editor of ESD.

507 **Acknowledgments**

508 We acknowledge the World Climate Research Programme, which, through its Working Group on Coupled  
509 Modelling, coordinated and promoted CMIP6. We thank the climate modelling groups for producing and making  
510 available their model output, the Earth System Grid Federation (ESGF) for archiving the data and providing  
511 access, and the multiple funding agencies who support CMIP6 and ESGF. We thank Richard Houghton of  
512 Woodwell Climate Research Center for providing the regional annual fluxes for LUC from HN2017, Eddy  
513 Robertson of Met Office, Vivek Arora of Canadian Centre for Climate Modelling and Analysis for providing  
514 additional information on the LUC implementation in ESMs. The IPSL-CM6 experiments were performed using  
515 the HPC resources of TGCC under the allocation 2020-A0080107732 (project gencmip6) provided by GENCI  
516 (Grand Equipement National de Calcul Intensif). This study benefited from State assistance managed by the  
517 National Research Agency in France under the Programme d'Investissements d'Avenir under the reference ANR-  
518 19-MPGA-0008. Our study was also supported by the European Union's Horizon 2020 research and innovation  
519 programme under grant agreement number 820829 for the "Constraining uncertainty of multi-decadal climate  
520 projections (CONSTRAIN)" project, by a grant from the French Ministry of the Ecological Transition as part of  
521 the Convention on financial support for climate services, by the Ministry of Education, Culture, Sports, Science  
522 and Technology (MEXT) of Japan (Integrated Research Program for Advancing Climate Models, grant no.  
523 JPMXD0717935715) and the Environment Research and Technology Development Fund (JPMEERF20192004)  
524 of the Environmental Restoration and Conservation Agency of Japan. RS acknowledges the European Union's  
525 Horizon 2020 research and innovation programme under grant agreement No 101003536 (ESM2025 – Earth  
526 System Models for the Future). RS acknowledges the support of the team in charge of the CNRM-CM climate  
527 model. Supercomputing time was provided by the Météo-France/DSI supercomputing center.

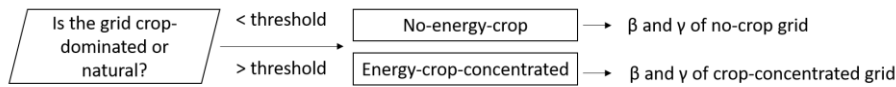


529 **Appendix**

530 **Text A1. Sensitivity study for deriving the crop-concentrated grid thresholds**

531 Neither IAMs nor ESMs provide BECCS-related LUC emissions. Separating BECCS-related emissions from all  
532 other LUC emissions is virtually impossible due to spatial heterogeneity and many complex factors that affect the  
533 bioenergy crop deployment.

534 ESMs do not distinguish second-generation bioenergy crops from other crops in CMIP6. Moreover, the cropland  
535 area in ESMs is defined at a sub-grid scale (i.e., on a fraction or tile of a grid box). Because land-use states (e.g.,  
536 forest, crops, pastures) vary in productivity and, thus, carbon uptakes and because modelling teams do not provide  
537 NBP estimates at the sub-grid level, to estimate the area and carbon fluxes of the biofuel crops in ESMs, we  
538 assume that all croplands deployed after the 2040s are for second-generation biofuel crops (Figure A1). We label  
539 the given grid of CMIP6 simulation outputs as crop-concentrated if the cropland fraction of the grid is larger than  
540 a given threshold derived via a sensitivity analysis (Figure A1).

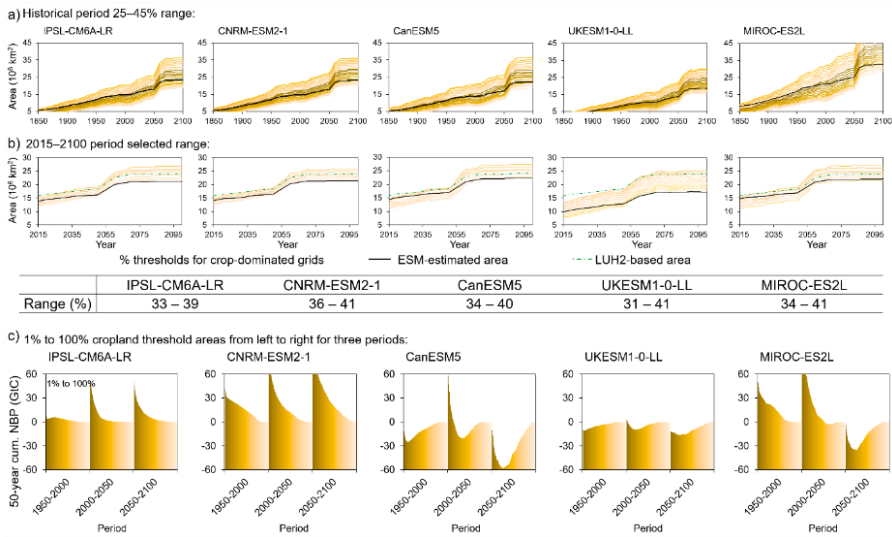


541  
542 **Figure A1: A schematic presentation of the sensitivity study for estimating the carbon-climate feedback parameters**  
543 **over the energy-crop-concentrated and no-energy-crop grids.**

544 We examined time-invariant cropland fraction thresholds ranging from 25% to 45% of the grid box area and  
545 selected a range of thresholds that best approximate the change in the total cropland area of each ESM in 2015–  
546 2100 (Figure A2). Here we choose the fitting period of 2015–2100 because a shorter period (2040–2100) would  
547 result in a lower threshold during the 2050–2060 period with a large global cropland increase. More specifically,  
548 we selected a range of thresholds with a 1%-step so that they intersect at least once either the global cropland area  
549 estimated by ESM itself or LUH2 data set from 2015 to 2100. Although, the selected ensembles of thresholds are  
550 time-invariant, the resultant cropland area increases. We find that for a later period (end of the 21<sup>st</sup> century), a  
551 higher threshold is required because both the spatial coverage (the number of grid boxes that have crops) and  
552 cropland concentration (a grid fraction of cropland) increases (Figure A2).

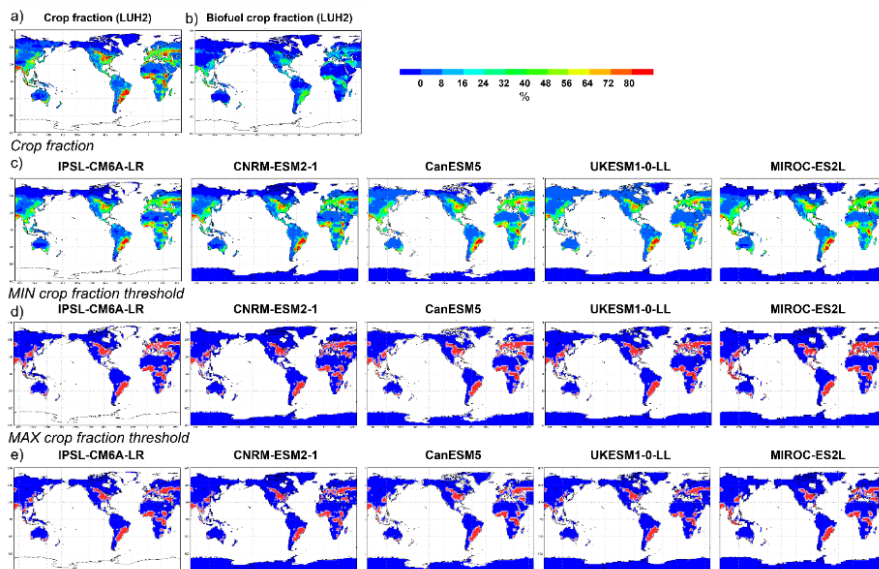
553 We confirmed the spatial distribution of the minimum and maximum selected thresholds of energy-crop-  
554 concentrated grids against sub-grid scale ESM and the LUH2 estimates of cropland area (Figure A3).





555

556 **Figure A2: (a) The cropland-fraction thresholds ranging from 25% to 45% of the grid box area analyzed in the**  
 557 **sensitivity study and (b) the selected (resultant) range of thresholds for identifying the energy-crop-concentrated area**  
 558 **with the selected range for each ESM indicated in the table. Panel (c) shows the cumulative NBP of the areas**  
 559 **corresponding to the range of cropland thresholds from 1 to 100% (left dark to right light color) in three periods.**



560 **Figure A3: Spatial variation of (a) grid cropland fraction (b) and second-generation bioenergy cropland fraction by**  
 561 **LUH2. Panel (c) shows the spatial variation of grid cropland fraction estimated by CMIP6 ESMs. The spatial variation**  
 562 **of the selected (d) minimum and (e) maximum thresholds (that intersect at least once either the global cropland area**  
 563 **estimated by ESM itself or LUH2 data set from 2015 to 2100 as shown in Figure A1) for estimating crop-concentrated**  
 564 **grids in 2100.**

566

567 **References**

- 568 Anderson, K. and Peters, G.: The trouble with negative emissions, *Science*, 354, 182,  
569 <https://doi.org/10.1126/science.aah4567>, 2016.
- 570 Arora, V. K., Katavouta, A., Williams, R. G., Jones, C. D., Brovkin, V., Friedlingstein, P., Schwinger, J., Bopp,  
571 L., Boucher, O., Cadule, P., Chamberlain, M. A., Christian, J. R., Delire, C., Fisher, R. A., Hajima, T., Ilyina, T.,  
572 Joetzjer, E., Kawamiya, M., Koven, C. D., Krasting, J. P., Law, R. M., Lawrence, D. M., Lenton, A., Lindsay, K.,  
573 Pongratz, J., Raddatz, T., Séférian, R., Tachiiri, K., Tjiputra, J. F., Wiltshire, A., Wu, T., and Ziehn, T.: Carbon-  
574 concentration and carbon-climate feedbacks in CMIP6 models and their comparison to CMIP5 models,  
575 *Biogeosciences*, 17, 4173–4222, <https://doi.org/10.5194/bg-17-4173-2020>, 2020.
- 576 Babin, A., Vaneekhaute, C., and Iliuta, M. C.: Potential and challenges of bioenergy with carbon capture and  
577 storage as a carbon-negative energy source: A review, *Biomass and Bioenergy*, 146, 105968,  
578 <https://doi.org/10.1016/j.biombioe.2021.105968>, 2021.
- 579 Bauer, N., Calvin, K., Emmerling, J., Fricko, O., Fujimori, S., Hilaire, J., Eom, J., Krey, V., Kriegler, E.,  
580 Mouratiadou, I., de Boer, H. S., van den Berg, M., Carrara, S., Daioglou, V., Drouet, L., Edmonds, J. E., Gernaat,  
581 D., Havlik, P., Johnson, N., Klein, D., Kyle, P., Marangoni, G., Masui, T., Pietzcker, R. C., Strubegger, M., Wise,  
582 M., Riahi, K., and van Vuuren, D. P.: Shared Socio-Economic Pathways of the Energy Sector – Quantifying the  
583 Narratives, *Glob. Environ. Change*, 42, 316–330, <https://doi.org/10.1016/j.gloenvcha.2016.07.006>, 2017.
- 584 Boucher, O., Servonnat, J., Albright, A. L., Aumont, O., Balkanski, Y., Bastrikov, V., Bekki, S., Bonnet, R., Bony,  
585 S., Bopp, L., Braconnot, P., Brockmann, P., Cadule, P., Caubel, A., Cheruy, F., Codron, F., Cozic, A., Cugnet,  
586 D., D'Andrea, F., Davini, P., Lavergne, C. de, Denvil, S., Deshayes, J., Devillers, M., Duchame, A., Dufresne,  
587 J.-L., Dupont, E., Éthé, C., Fairhead, L., Falletti, L., Flavoni, S., Foujols, M.-A., Gardoll, S., Gastineau, G.,  
588 Ghattas, J., Grandpeix, J.-Y., Guenet, B., Guez, L. E., Guilyardi, E., Guimberteau, M., Hauglustaine, D., Hourdin,  
589 F., Idelkadi, A., Joussaume, S., Kageyama, M., Khodri, M., Krinner, G., Lebas, N., Levavasseur, G., Lévy, C., Li,  
590 L., Lott, F., Lurton, T., Luysaert, S., Madec, G., Madeleine, J.-B., Maignan, F., Marchand, M., Marti, O., Mellul,  
591 L., Meurdesoif, Y., Mignot, J., Musat, I., Ottlé, C., Peylin, P., Planton, Y., Polcher, J., Rio, C., Rochetin, N.,  
592 Rousset, C., Sepulchre, P., Sima, A., Swingedouw, D., Thiéblemont, R., Traore, A. K., Vancoppenolle, M., Vial,  
593 J., Vialard, J., Viovy, N., and Vuichard, N.: Presentation and Evaluation of the IPSL-CM6A-LR Climate Model,  
594 *J. Adv. Model Earth Sy.*, 12, e2019MS002010, <https://doi.org/10.1029/2019MS002010>, 2020.
- 595 [Boysen, L.ena R., Victor-Brovkin, V., David-Wärilind, D., Daniele-Peano, D., Anne-Sofie Lansø, A.S., Christine](#)  
596 [Delire, C., Eleanor-Burke, E., Christopher-Poeplau, C., and Axel Don., A.: "Evaluation of soil carbon dynamics](#)  
597 [after forest cover change in CMIP6 land models using chronosequences." \*Environ. Res. Lett. Environmental\*](#)  
598 [Research Letters](#) 16, no. 7 (2021): 074030. <https://doi.org/10.1088/1748-9326/ac0be1>, 2021
- 599
- 600 [Brovkin, V., Boysen, L., Wärilind, D., Peano, D., Lansø, A. S., Delire, C., Burke, E., Poeplau, C., and Don, A.:](#)  
601 [Evaluation of soil carbon dynamics after land use change in CMIP6 land models using chronosequences, EGU](#)  
602 [General Assembly 2021, online, 19–30 Apr 2021, EGU21-12561, \[https://doi.org/10.5194/egusphere-egu21-\]\(https://doi.org/10.5194/egusphere-egu21-12561\)](#)  
603 [12561, 2021.](#) Campbell, J. E., Lobell, D. B., Genova, R. C., and Field, C. B.: The global potential of bioenergy  
604 on abandoned agriculture lands, *Environ Sci Technol.*, 42, 5791–5794, <https://doi.org/10.1021/es800052w>, 2008.
- 605 Canadell, J. G. and Schulze, E. D.: Global potential of biospheric carbon management for climate mitigation, *Nat.*  
606 *Commun.*, 5, 1–12, <https://doi.org/10.1038/ncomms6282>, 2014.
- 607 Clair, S. S., Hillier, J., and Smith, P.: Estimating the pre-harvest greenhouse gas costs of energy crop production,  
608 *Biomass Bioenerg.*, 32, 442–452, <https://doi.org/10.1016/j.biombioe.2007.11.001>, 2008.
- 609 Dooley, K., Christoff, P., and Nicholas, K. A.: Co-producing climate policy and negative emissions: trade-offs  
610 for sustainable land-use, *Global Sustainability*, 1, <https://doi.org/10.1017/sus.2018.6>, 2018.
- 611 Erb, K.-H., Fetzel, T., Plutzer, C., Kastner, T., Lauk, C., Mayer, A., Niedertscheider, M., Kömer, C., and Haberl,  
612 H.: Biomass turnover time in terrestrial ecosystems halved by land use, *Nature Geoscience*, 9, 674–678,  
613 <https://doi.org/10.1038/ngeo2782>, 2016.

Mis en forme : Normal, Espace Après : 12 pt

614 Fargione, J., Hill, J., Tilman, D., Polasky, S., and Hawthorne, P.: Land Clearing and the Biofuel Carbon Debt,  
615 Science, 319, 1235, <https://doi.org/10.1126/science.1152747>, 2008.

616 Friedlingstein, P., Cox, P., Betts, R., Bopp, L., von Bloh, W., Brovkin, V., Cadule, P., Doney, S., Eby, M., Fun  
617 I., Bala, G., John, J., Jones, C., Joos, F., Kato, T., Kawamiya, M., Knorr, W., Lindsay, K., Matthews, H. D.,  
618 Raddatz, T., Rayner, P., Reick, C., Roeckner, E., Schnitzler, K.-G., Schnur, R., Strassmann, K., Weaver, A. J.,  
619 Yoshikawa, C., and Zeng, N.: Climate–Carbon Cycle Feedback Analysis: Results from the C4MIP Model  
620 Intercomparison, *J. Climate*, 19, 3337–3353, <https://doi.org/10.1175/JCLI3800.1>, 2006.

621 Friedlingstein, P., O’Sullivan, M., Jones, M. W., Andrew, R. M., Hauck, J., Olsen, A., Peters, G. P., Peters, W.,  
622 Pongratz, J., Sitch, S., Le Quééré, C., Canadell, J. G., Ciais, P., Jackson, R. B., Alin, S., Aragão, L. E. O. C., Ameth,  
623 A., Arora, V., Bates, N. R., Becker, M., Benoit-Cattin, A., Bittig, H. C., Bopp, L., Bultan, S., Chandra, N.,  
624 Chevallier, F., Chini, L. P., Evans, W., Florentie, L., Forster, P. M., Gasser, T., Gehlen, M., Gilfillan, D.,  
625 Gkritzalis, T., Gregor, L., Gruber, N., Harris, I., Hartung, K., Haverd, V., Houghton, R. A., Ilyina, T., Jain, A. K.,  
626 Joetzjer, E., Kadono, K., Kato, E., Kitidis, V., Korsbakken, J. I., Landschützer, P., Lefèvre, N., Lenton, A., Lienert,  
627 S., Liu, Z., Lombardozi, D., Marland, G., Metz, N., Munro, D. R., Nabel, J. E. M. S., Nakaoka, S.-I., Niwa, Y.,  
628 O’Brien, K., Ono, T., Palmer, P. I., Pierrot, D., Poulter, B., Resplandy, L., Robertson, E., Rödenbeck, C.,  
629 Schwinger, J., Séférian, R., Skjelvan, I., Smith, A. J. P., Sutton, A. J., Tanhua, T., Tans, P. P., Tian, H., Tilbrook,  
630 B., van der Werf, G., Vuichard, N., Walker, A. P., Wanninkhof, R., Watson, A. J., Willis, D., Wiltshire, A. J.,  
631 Yuan, W., Yue, X., and Zaehle, S.: Global Carbon Budget 2020, *Earth Syst. Sci. Data*, 12, 3269–3340,  
632 <https://doi.org/10.5194/essd-12-3269-2020>, 2020.

633 Gasser, T. and Ciais, P.: A theoretical framework for the net land-to-atmosphere CO<sub>2</sub> flux and its implications in  
634 the definition of “emissions from land-use change”, *Earth Syst. Dynam.*, 4, 171–186, <https://doi.org/10.5194/esd-4-171-2013>, 2013.

636 Gasser, T., Crepin, L., Quilcaille, Y., Houghton, R. A., Ciais, P., and Obersteiner, M.: Historical CO<sub>2</sub> emissions  
637 from land use and land cover change and their uncertainty, *Biogeosciences*, 17, 4075–4101,  
638 <https://doi.org/10.5194/bg-17-4075-2020>, 2020.

639 Gibbs, H. K., Johnston, M., Foley, J. A., Holloway, T., Monfreda, C., Ramankutty, N., and Zaks, D.: Carbon  
640 payback times for crop-based biofuel expansion in the tropics: the effects of changing yield and technology,  
641 *Environ Res Lett.*, 3, 034001, <https://doi.org/10.1088/1748-9326/3/3/034001>, 2008.

642 Gregory, J. M., Jones, C. D., Cadule, P., and Friedlingstein, P.: Quantifying Carbon Cycle Feedbacks, *J. Climate*,  
643 22, 5232–5250, <https://doi.org/10.1175/2009JCLI2949.1>, 2009.

644 Hajima, T., Watanabe, M., Yamamoto, A., Tatebe, H., Noguchi, M. A., Abe, M., Ohgaito, R., Ito, A., Yamazaki,  
645 D., Okajima, H., Ito, A., Takata, K., Ogochi, K., Watanabe, S., and Kawamiya, M.: Development of the MIROC-  
646 ES2L Earth system model and the evaluation of biogeochemical processes and feedbacks, *Geosci. Model Dev.*,  
647 13, 2197–2244, <https://doi.org/10.5194/gmd-13-2197-2020>, 2020.

648 Hansis, E., Davis, S. J., and Pongratz, J.: Relevance of methodological choices for accounting of land use change  
649 carbon fluxes, *Global. Biogeochem. Cy.*, 29, 1230–1246, <https://doi.org/10.1002/2014GB004997>, 2015.

650 Harper, A. B., Powell, T., Cox, P. M., House, J., Huntingford, C., Lenton, T. M., Sitch, S., Burke, E., Chadburn,  
651 S. E., Collins, W. J., Comyn-Platt, E., Daioglou, V., Doelman, J. C., Hayman, G., Robertson, E., van Vuuren, D.,  
652 Wiltshire, A., Webber, C. P., Bastos, A., Boysen, L., Ciais, P., Devaraju, N., Jain, A. K., Krause, A., Poulter, B.,  
653 and Shu, S.: Land-use emissions play a critical role in land-based mitigation for Paris climate targets, *Nat.*  
654 *Commun.*, 9, 2938, <https://doi.org/10.1038/s41467-018-05340-z>, 2018.

655 Heck, V., Gerten, D., Lucht, W., and Popp, A.: Biomass-based negative emissions difficult to reconcile with  
656 planetary boundaries, *Nat. Clim. Change*, 8, 151–155, <https://doi.org/10.1038/s41558-017-0064-y>, 2018.

657 Houghton, R. A. and Nassikas, A. A.: Global and regional fluxes of carbon from land use and land cover change  
658 1850–2015, *Global. Biogeochem. Cy.*, 31, 456–472, <https://doi.org/10.1002/2016GB005546>, 2017.

659 Hurtt, G. C., Chini, L., Sahajpal, R., Frohling, S., Bodirsky, B. L., Calvin, K., Doelman, J. C., Fisk, J., Fujimori,  
660 S., Goldewijk, K. K., Hasegawa, T., Havlik, P., Heinemann, A., Humpenöder, F., Jungclaus, J., Kaplan, J.,  
661 Kennedy, J., Kristzin, T., Lawrence, D., Lawrence, P., Ma, L., Mertz, O., Pongratz, J., Popp, A., Poulter, B., Riahi,

662 K., Shevliakova, E., Stehfest, E., Thornton, P., Tubiello, F. N., van Vuuren, D. P., and Zhang, X.: Harmonization  
663 of Global Land-Use Change and Management for the Period 850-2100 (LUH2) for CMIP6, *Geosci Model Dev.*,  
664 1–65, <https://doi.org/10.5194/gmd-2019-360>, 2020.

665 Jones, C. D., Arora, V., Friedlingstein, P., Bopp, L., Brovkin, V., Dunne, J., Graven, H., Hoffman, F., Ilyina, T.,  
666 John, J. G., Jung, M., Kawamiya, M., Koven, C., Pongratz, J., Raddatz, T., Randerson, J. T., and Zaehle, S.:  
667 C4MIP - The Coupled Climate–Carbon Cycle Model Intercomparison Project: experimental protocol for CMIP6,  
668 *Geosci. Model Dev.*, 9, 2853–2880, <https://doi.org/10.5194/gmd-9-2853-2016>, 2016a.

669 Jones, C. D., Ciais, P., Davis, S. J., Friedlingstein, P., Gasser, T., Peters, G. P., Rogelj, J., van Vuuren, D. P.,  
670 Canadell, J. G., Cowie, A., Jackson, R. B., Jonas, M., Kriegler, E., Littleton, E., Lowe, J. A., Milne, J., Shrestha,  
671 G., Smith, P., Torvanger, A., and Wiltshire, A.: Simulating the Earth system response to negative emissions,  
672 *Environ. Res. Lett.*, 11, 095012, <https://doi.org/10.1088/1748-9326/11/9/095012>, 2016b.

673 Jones, M. B. and Albanito, F.: Can biomass supply meet the demands of bioenergy with carbon capture and storage  
674 (BECCS)?, *Glob. Change Biol.*, 26, 5358–5364, <https://doi.org/10.1111/gcb.15296>, 2020.

675 Keller, D. P., Lenton, A., Scott, V., Vaughan, N. E., Bauer, N., Ji, D., Jones, C. D., Kravitz, B., Muri, H., and  
676 Zickfeld, K.: The Carbon Dioxide Removal Model Intercomparison Project (CDRMIP): rationale and  
677 experimental protocol for CMIP6, *Geosci. Model Dev.*, 11, 1133–1160, [https://doi.org/10.5194/gmd-11-1133-](https://doi.org/10.5194/gmd-11-1133-2018)  
678 2018, 2018.

679 Krause, A., Pugh, T. A. M., Bayer, A. D., Li, W., Leung, F., Bondeau, A., Doelman, J. C., Humpenöder, F.,  
680 Anthoni, P., Bodirsky, B. L., Ciais, P., Müller, C., Murray-Tortarolo, G., Olin, S., Popp, A., Sitch, S., Stehfest,  
681 E., and Arneth, A.: Large uncertainty in carbon uptake potential of land-based climate-change mitigation efforts,  
682 *Glob. Change Biol.*, 24, 3025–3038, <https://doi.org/10.1111/gcb.14144>, 2018.

683 Kriegler, E., Bauer, N., Popp, A., Humpenöder, F., Leimbach, M., Strefler, J., Baumstark, L., Bodirsky, B. L.,  
684 Hilaire, J., Klein, D., Mouratiadou, I., Weindl, I., Bertram, C., Dietrich, J.-P., Luderer, G., Pehl, M., Pietzcker, R.,  
685 Piontek, F., Lotze-Campen, H., Biewald, A., Bonsch, M., Giannousakis, A., Kreidenweis, U., Müller, C., Rolinski,  
686 S., Schultes, A., Schwanitz, J., Stevanovic, M., Calvin, K., Emmerling, J., Fujimori, S., and Edenhofer, O.: Fossil-  
687 fueled development (SSP5): An energy and resource intensive scenario for the 21st century, *Glob. Environ.*  
688 *Change*, 42, 297–315, <https://doi.org/10.1016/j.gloenvcha.2016.05.015>, 2017.

689 Li, W., Ciais, P., Han, M., Zhao, Q., Chang, J., Goll, D. S., Zhu, L., and Wang, J.: Bioenergy Crops for Low  
690 Warming Targets Require Half of the Present Agricultural Fertilizer Use, *Environ. Sci. Technol.*, 55, 10654–  
691 10661, <https://doi.org/10.1021/acs.est.1c02238>, 2021.

692 Liddicoat, S. K., Wiltshire, A. J., Jones, C. D., Arora, V. K., Brovkin, V., Cadule, P., Hajima, T., Lawrence, D.  
693 M., Pongratz, J., and Schwinger, J.: Compatible Fossil Fuel CO<sub>2</sub> Emissions in the CMIP6 Earth System Models’  
694 Historical and Shared Socioeconomic Pathway Experiments of the Twenty-First Century, *J. Climate*, 34, 2853–  
695 2875, <https://doi.org/10.1175/JCLI-D-19-0991.1>, 2021.

696 Meinshausen, M., Nicholls, Z. R. J., Lewis, J., Gidden, M. J., Vogel, E., Freund, M., Beyerle, U., Gessner, C.,  
697 Nauels, A., Bauer, N., Canadell, J. G., Daniel, J. S., John, A., Krummel, P. B., Luderer, G., Meinshausen, N.,  
698 Montzka, S. A., Rayner, P. J., Reimann, S., Smith, S. J., van den Berg, M., Velders, G. J. M., Vollmer, M. K., and  
699 Wang, R. H. J.: The shared socio-economic pathway (SSP) greenhouse gas concentrations and their extensions to  
700 2500, *Geosci. Model Dev.*, 13, 3571–3605, <https://doi.org/10.5194/gmd-13-3571-2020>, 2020.

701 Melnikova, I., Boucher, O., Cadule, P., Ciais, P., Gasser, T., Quilcaille, Y., Shiogama, H., Tachiiri, K., Yokohata,  
702 T., and Tanaka, K.: Carbon cycle response to temperature overshoot beyond 2 °C – an analysis of CMIP6 models,  
703 *Earth’s Future*, 9, e2020EF001967, <https://doi.org/10.1029/2020EF001967>, 2021.

704 Mohr, A. and Raman, S.: Lessons from first generation biofuels and implications for the sustainability appraisal  
705 of second generation biofuels, *Energy Policy*, 63, 114–122, <https://doi.org/10.1016/j.enpol.2013.08.033>, 2013.

706 O’Neill, B. C., Tebaldi, C., Van Vuuren, D. P., Eyring, V., Friedlingstein, P., Hurtt, G., Knutti, R., Kriegler, E.,  
707 Lamarque, J. F., Lowe, J., Meehl, G. A., Moss, R., Riahi, K., and Sanderson, B. M.: The Scenario Model  
708 Intercomparison Project (ScenarioMIP) for CMIP6, *Geosci. Model Dev.*, 9, [https://doi.org/10.5194/gmd-9-3461-](https://doi.org/10.5194/gmd-9-3461-2016)  
709 2016, 2016.

710 Pongratz, J., Reick, C. H., Houghton, R. A., and House, J. I.: Terminology as a key uncertainty in net land use  
711 and land cover change carbon flux estimates, *Earth Syst. Dynam.*, 5, 177–195, [https://doi.org/10.5194/esd-5-177-](https://doi.org/10.5194/esd-5-177-2014)  
712 2014, 2014.

713 Popp, A., Calvin, K., Fujimori, S., Havlik, P., Humpenöder, F., Stehfest, E., Bodirsky, B. L., Dietrich, J. P.,  
714 Doelmann, J. C., Gusti, M., Hasegawa, T., Kyle, P., Obersteiner, M., Tabeau, A., Takahashi, K., Valin, H.,  
715 Waldhoff, S., Weindl, I., Wise, M., Kriegler, E., Lotze-Campen, H., Fricko, O., Riahi, K., and van Vuuren, D. P.:  
716 Land-use futures in the shared socio-economic pathways, *Glob. Environ. Change*, 42, 331–345,  
717 <https://doi.org/10.1016/j.gloenvcha.2016.10.002>, 2017.

718 Riahi, K., van Vuuren, D. P., Kriegler, E., Edmonds, J., O'Neill, B. C., Fujimori, S., Bauer, N., Calvin, K., Dellink,  
719 R., Fricko, O., Lutz, W., Popp, A., Cuaresma, J. C., Samir, K. C., Leimbach, M., Jiang, L., Kram, T., Rao, S.,  
720 Emmerling, J., Ebi, K., Hasegawa, T., Havlik, P., Humpenöder, F., Silva, L. A. D., Smith, S., Stehfest, E., Bosetti,  
721 V., Eom, J., Gemaat, D., Masui, T., Rogelj, J., Strefler, J., Drouet, L., Krey, V., Luderer, G., Hamsen, M.,  
722 Takahashi, K., Baumstark, L., Doelman, J. C., Kainuma, M., Klimont, Z., Marangoni, G., Lotze-Campen, H.,  
723 Obersteiner, M., Tabeau, A., and Tavoni, M.: The Shared Socioeconomic Pathways and their energy, land use,  
724 and greenhouse gas emissions implications: An overview, *Glob. Environ. Change*, 42, 153–168,  
725 <https://doi.org/10.1016/j.gloenvcha.2016.05.009>, 2017.

726 Rogelj, J., Shindell, D., Jiang, K., Fifita, S., Forster, P., Ginzburg, V., Handa, C., Kheshgi, H., Kobayashi, S.,  
727 Kriegler, E., Mundaca, L., Séférian, R., Vilarino, M. V., Calvin, K., de Oliveira de Portugal Pereira, J. C.,  
728 Edelenbosch, O., Emmerling, J., Fuss, S., Gasser, T., Gillett, N., He, C., Hertwich, E., Höglund-Isaksson, L.,  
729 Huppmann, D., Luderer, G., Markandya, A., Meinshausen, M., McCollum, D., Millar, R., Popp, A., Purohit, P.,  
730 Riahi, K., Ribes, A., Saunders, H., Schädel, C., Smith, C., Smith, P., Trutnevyte, E., Xu, Y., Zhou, W., Zickfeld,  
731 K., *Mitigation Pathways Compatible with 1.5°C in the Context of Sustainable Development*. - In: Masson-  
732 Delmotte, V., Zhai, P., Pörtner, H. O., Roberts, D., Skea, J., Shukla, P. R., Pirani, A., Moufouma-Okia, W., Péan,  
733 C., Pidcock, R., Connors, S., Matthews, J. B. R., Chen, Y., Zhou, X., Zhou, M. I., Lonnoy, E., Maycock, T.,  
734 Tignor, M., Waterfield, T. (Eds.), *Global warming of 1.5 °C*, (IPCC Special Report), Geneva: Intergovernmental  
735 Panel on Climate Change, 93-174, 2018.

736 Schueler, V., Weddige, U., Beringer, T., Gamba, L., and Lamers, P.: Global biomass potentials under  
737 sustainability restrictions defined by the European Renewable Energy Directive 2009/28/EC, *GCB Bioenergy*, 5,  
738 652–663, <https://doi.org/10.1111/gcbb.12036>, 2013.

739 Schwinger, J. and Tjiputra, J.: Ocean Carbon Cycle Feedbacks Under Negative Emissions, *Geophys. Res. Lett.*,  
740 45, 5062–5070, <https://doi.org/10.1029/2018GL077790>, 2018.

741 Séférian, R., Rocher, M., Guivarch, C., and Colin, J.: Constraints on biomass energy deployment in mitigation  
742 pathways: the case of water scarcity, *Environ. Res. Lett.*, 13, 054011, <https://doi.org/10.1088/1748-9326/aabcd7>,  
743 2018.

744 Séférian, R., Nabat, P., Michou, M., Saint-Martin, D., Voldoire, A., Colin, J., Decharme, B., Delire, C., Berthet,  
745 S., Chevallier, M., Sénési, S., Franchisteguy, L., Vial, J., Mallet, M., Joetzjer, E., Geoffroy, O., Guérémy, J.-F.,  
746 Moine, M.-P., Msadek, R., Ribes, A., Rocher, M., Roebrig, R., Salas-y-Méla, D., Sanchez, E., Terray, L., Valcke,  
747 S., Waldman, R., Aumont, O., Bopp, L., Deshayes, J., Été, C., and Madec, G.: Evaluation of CNRM Earth  
748 System Model, CNRM-ESM2-1: Role of Earth System Processes in Present-Day and Future Climate, *J. Adv.  
749 Model Earth Sy.*, 11, 4182–4227, <https://doi.org/10.1029/2019MS001791>, 2019.

750 Sellar, A. A., Jones, C. G., Mulcahy, J. P., Tang, Y., Yool, A., Wiltshire, A., O'Connor, F. M., Stringer, M., Hill,  
751 R., Palmieri, J., Woodward, S., Mora, L. de, Kuhlbrodt, T., Rumbold, S. T., Kelley, D. I., Ellis, R., Johnson, C.  
752 E., Walton, J., Abraham, N. L., Andrews, M. B., Andrews, T., Archibald, A. T., Berthou, S., Burke, E., Blockley,  
753 E., Carslaw, K., Dalvi, M., Edwards, J., Folberth, G. A., Gedney, N., Griffiths, P. T., Harper, A. B., Hendry, M.  
754 A., Hewitt, A. J., Johnson, B., Jones, A., Jones, C. D., Keeble, J., Liddicoat, S., Morgenstern, O., Parker, R. J.,  
755 Predoi, V., Robertson, E., Siahann, A., Smith, R. S., Swaminathan, R., Woodhouse, M. T., Zeng, G., and  
756 Zerroukat, M.: UKESM1: Description and Evaluation of the U.K. Earth System Model, *J. Adv. Model Earth Sy.*,  
757 11, 4513–4558, <https://doi.org/10.1029/2019MS001739>, 2019.

758 Shukla, P. R., Skea, J., Calvo Buendia, E., Masson-Delmotte, V., Pörtner, H. O., Roberts, D. C., Zhai, P., Slade,  
759 R., Connors, S., and Van Diemen, R.: IPCC, 2019: Climate Change and Land: an IPCC special report on climate

760 change, desertification, land degradation, sustainable land management, food security, and greenhouse gas fluxes  
761 in terrestrial ecosystems, 2019.

762 Smith, P., Davis, S. J., Creutzig, F., Fuss, S., Minx, J., Gabrielle, B., Kato, E., Jackson, R. B., Cowie, A., and  
763 Kriegler, E.: Biophysical and economic limits to negative CO<sub>2</sub> emissions, *Nat. Clim. Change*, 6, 42–50,  
764 <https://doi.org/10.1038/nclimate2870>, 2016.

765 Swart, N. C., Cole, J. N. S., Kharin, V. V., Lazare, M., Scinocca, J. F., Gillett, N. P., Anstey, J., Arora, V.,  
766 Christian, J. R., Hanna, S., Jiao, Y., Lee, W. G., Majaess, F., Saenko, O. A., Seiler, C., Seinen, C., Shao, A.,  
767 Sigmond, M., Solheim, L., von Salzen, K., Yang, D., and Winter, B.: The Canadian Earth System Model version  
768 5 (CanESM5.0.3), *Geosci. Model Dev.*, 12, 4823–4873, <https://doi.org/10.5194/gmd-12-4823-2019>, 2019.

769 Tanaka, K., Boucher, O., Ciais, P., Johansson, D. J. A., and Morfeldt, J.: Cost-effective implementation of the  
770 Paris Agreement using flexible greenhouse gas metrics, *Sci Adv*, 7, eabf9020,  
771 <https://doi.org/10.1126/sciadv.abf9020>, 2021.

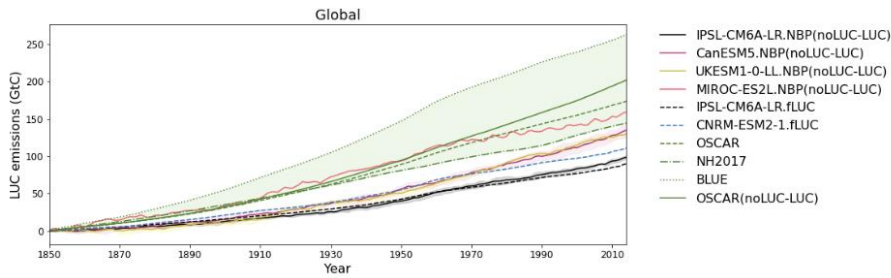
772 Whitaker, J., Field, J. L., Bernacchi, C. J., Cerri, C. E. P., Ceulemans, R., Davies, C. A., DeLucia, E. H., Donnison,  
773 I. S., McCalmont, J. P., Paustian, K., Rowe, R. L., Smith, P., Thomley, P., and McNamara, N. P.: Consensus,  
774 uncertainties and challenges for perennial bioenergy crops and land use, *GCB Bioenergy*, 10, 150–164,  
775 <https://doi.org/10.1111/gcbb.12488>, 2018.

776 Wu, D., Piao, S., Zhu, D., Wang, X., Ciais, P., Bastos, A., Xu, X., and Xu, W.: Accelerated terrestrial ecosystem  
777 carbon turnover and its drivers, *Globa. Change Biol.*, 26, 5052–5062, <https://doi.org/10.1111/gcb.15224>, 2020.

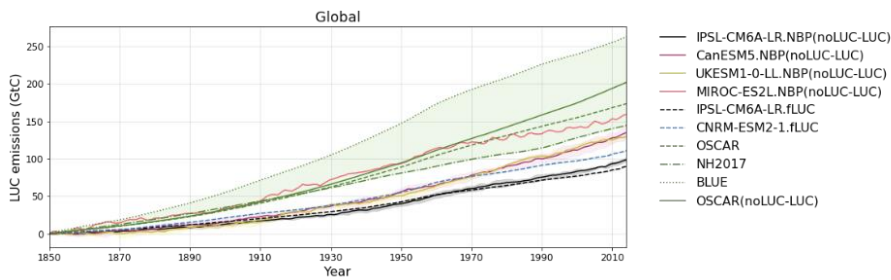
778 [Zhang, X., Wang, Y.P., Rayner, P.J., Ciais, P., Huang, K., Luo, Y., Piao, S., Wang, Z., Xia, J., Zhao, W. and](https://doi.org/10.1038/s41467-021-22392-w)  
779 [Zheng, X.. A small climate-amplifying effect of climate-carbon cycle feedback, \*Nature communications\*, 12\(1\):](https://doi.org/10.1038/s41467-021-22392-w)  
780 [1-11, https://doi.org/10.1038/s41467-021-22392-w, 2021.](https://doi.org/10.1038/s41467-021-22392-w)



790



791

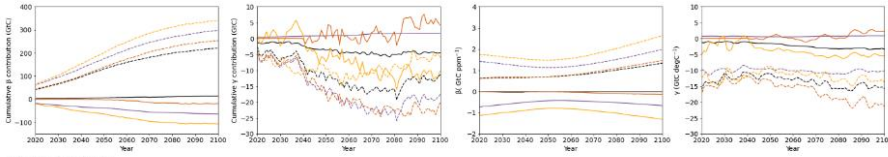


792

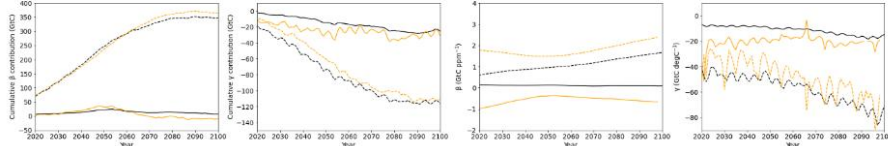
793 **Figure 12:** Evaluation of cumulative global LUC emissions by ESMs against three bookkeeping models. LUC emissions  
794 are defined by two methods: 1) the difference in NBP between simulations with and without LUC (solid lines) and 2)  
795 the “fLUC” variable provided in CMIP6 (dashed lines). The estimates of bookkeeping approach using OSCAR are  
796 shown for cases with (noLUC-LUC) and without LASC). The range of bookkeeping models is shaded green.



a) IPSL-CM6A-LR



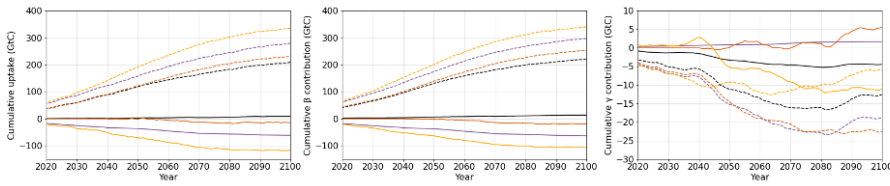
b) MIROC ES2L



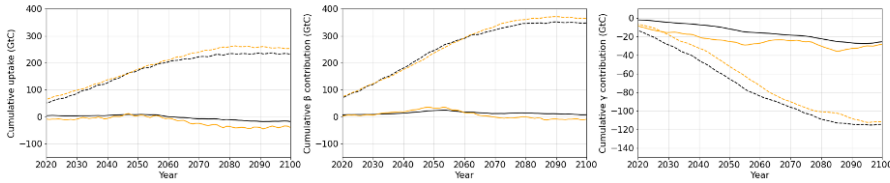
— fLUC  
 — Cropland threshold  
 — Two simulations 1850  
 — Two simulations 2040

Solid lines are LUC- (or crop-concentrated) and dashed lines are noLUC- (no-crop) contributions  
 Y-axis differ

a) IPSL-CM6A-LR



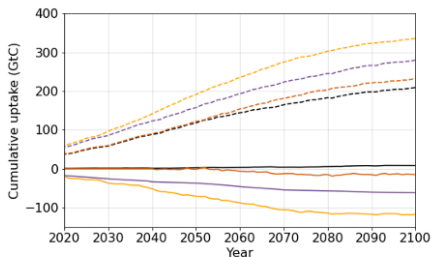
b) MIROC ES2L



**LUC- (crop-concentrated):**  
 — fLUC  
 — Cropland threshold  
 — Two simulations 1850  
 — Two simulations 2040

**noLUC- (no-crop):**  
 - - - fLUC  
 - - - Cropland threshold  
 - - - Two simulations 1850  
 - - - Two simulations 2040

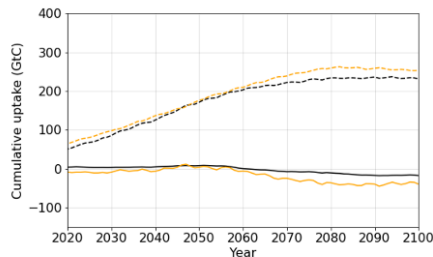
a) IPSL-CM6A-LR



LUC- (crop-concentrated):

- fLUC
- Cropland threshold
- Two simulations 1850
- Two simulations 2040

b) MIROC ES2L

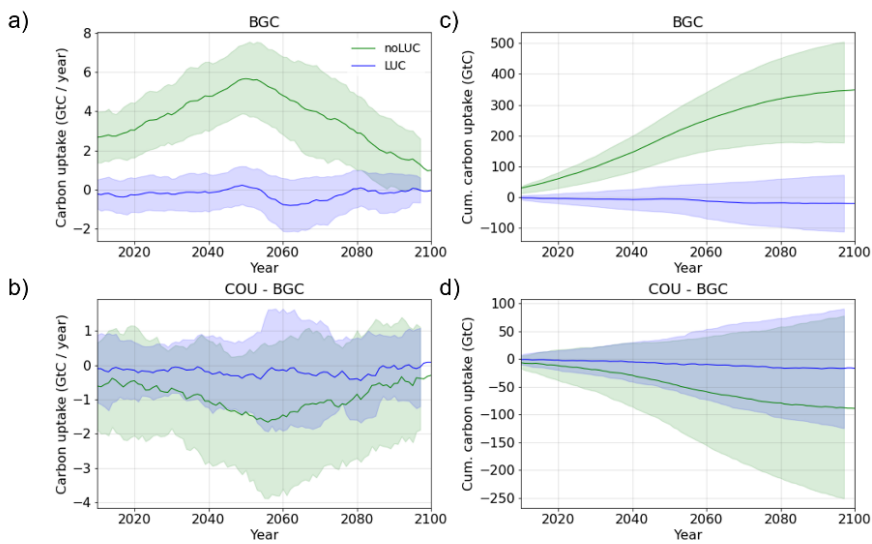


noLUC- (no-crop):

- fLUC
- Cropland threshold
- Two simulations 1850
- Two simulations 2040

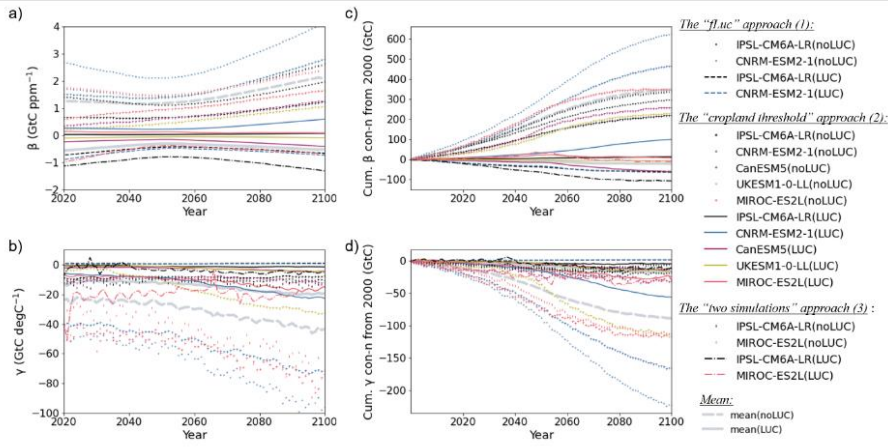
799 **Figure 23: Differences in the impact of LUC on carbon cycle estimated by three approaches by (a) IPSL-CM6A-LR**  
 800 **and (b) MIROC-ES2L. From left to right: eCumulative carbon uptake, and  $\beta$  and  $\gamma$  contributions to land carbon**  
 801 **uptake from year 2000, uptake, and global land  $\beta$  and  $\gamma$  feedback parameters in LUC-concentrated (solid lines) and**  
 802 **noLUC (dashed lines) ecosystems estimated by three approaches by (a) IPSL-CM6A-LR and (b) MIROC-ES2L.**  
 803

804



805

806



807

808

809

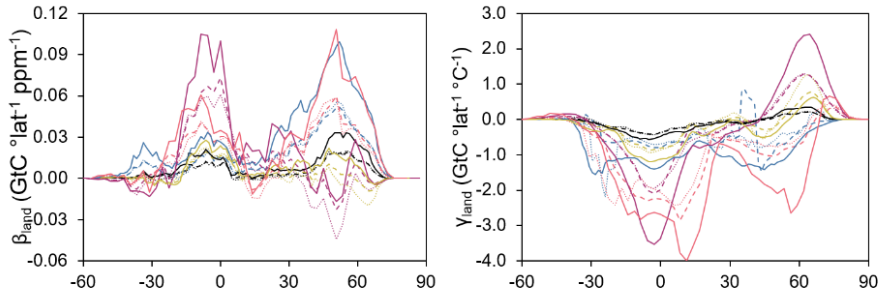
810

811

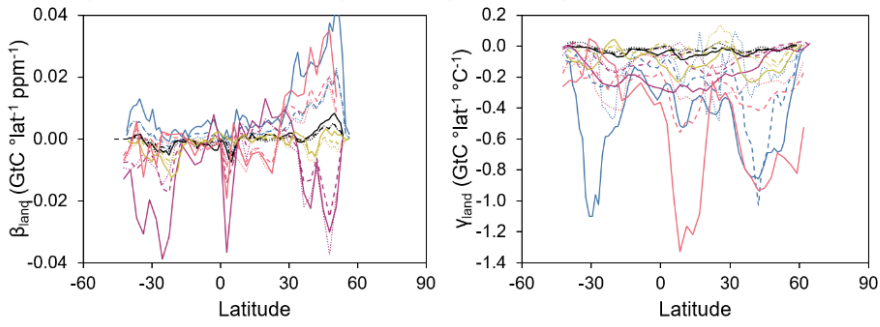
812

**Figure 34:** Interannual variation of global (a, b) feedback parameters and carbon uptake and (c, d) cumulative carbon uptake in LUC or crop-concentrated and noLUC or no-crop ecosystems by given as mean and standard deviation (shaded area) of five ESMs and three approaches. The panels a and c show BGC simulation outputs, and the panels b and d show the difference in COU and BGC simulation outputs.

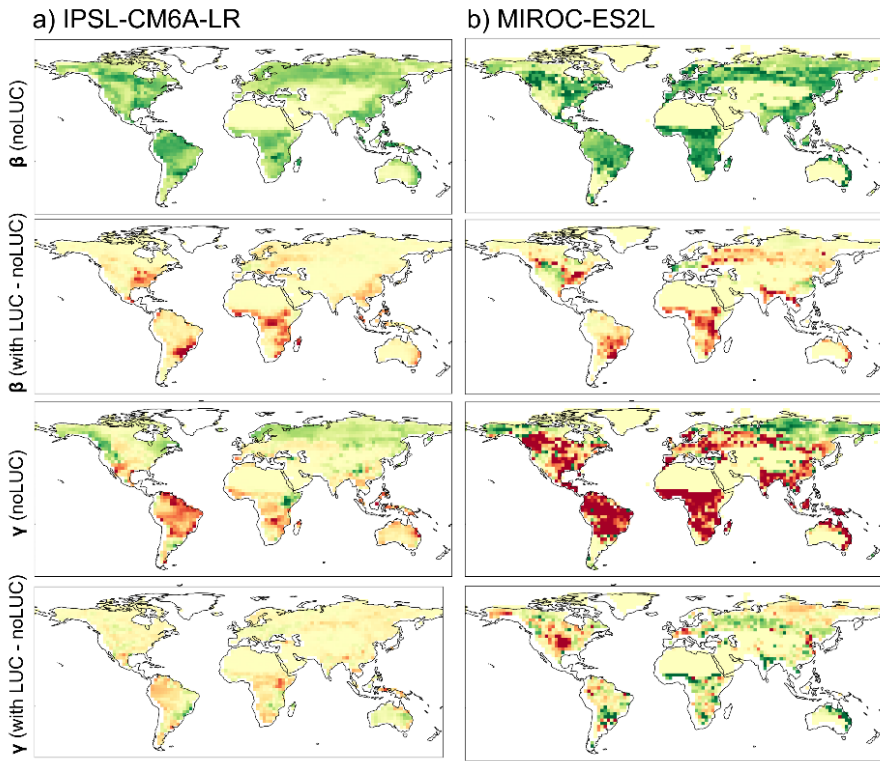
a) Global:



b) Crop-concentrated areas (as in the year 2100):

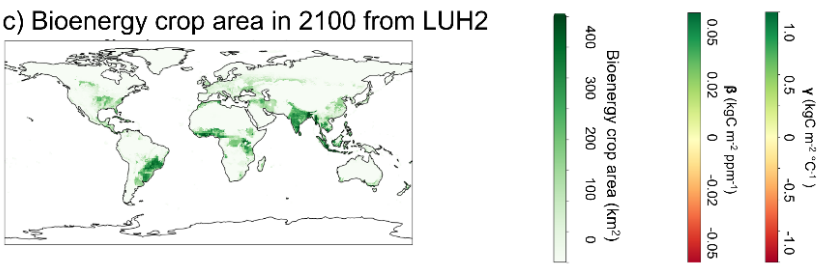


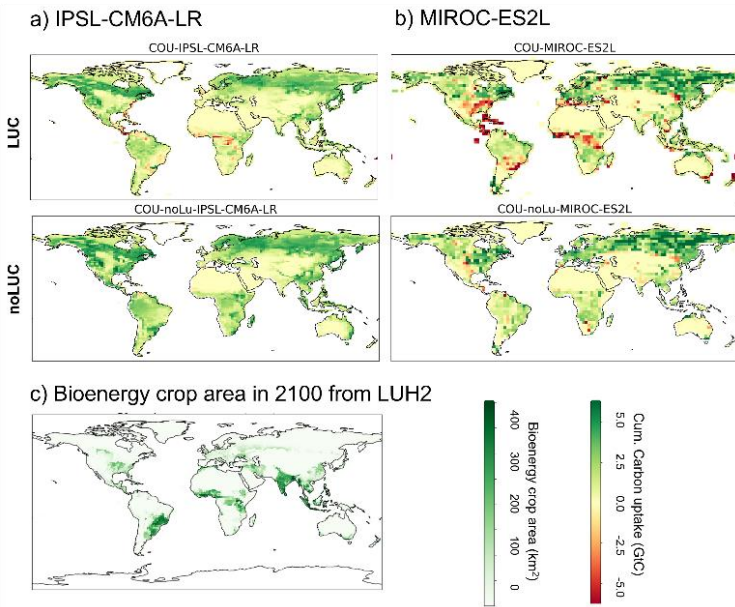
— IPSL-CM6A-LR — CNRM-ESM2-1 — CanESM5 — UKESM1-0-LL — MIROC-ES2L  
 ..... 2030–2040 mean - - - - 2040–2050 mean ——— 2090–2100 mean



Negative values of (with LUC – noLUC) differences mean less sink / larger source due to LUC

c) Bioenergy crop area in 2100 from LUH2





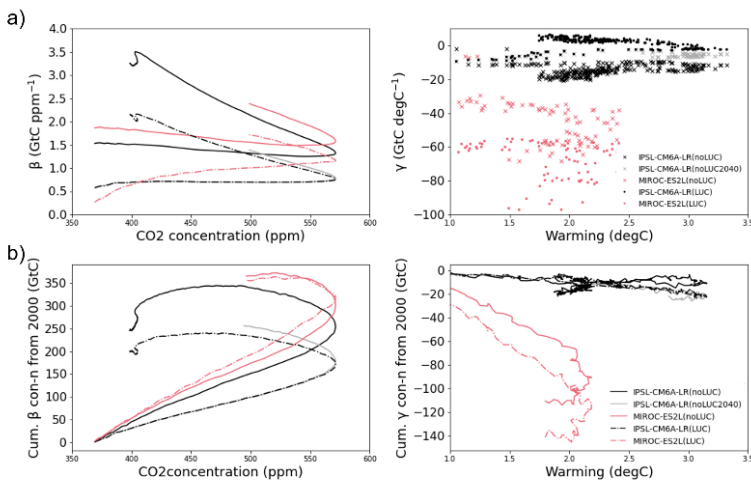
816

817 **Figure 54: Spatial variations of the  $\beta$  and  $\gamma$  parameters cumulative over 2040 – 2100 period carbon uptake**  
 818 **by (a) IPSL-CM6A-LR and (b) MIROC-ES2L given for the noLUC fully coupled simulations and for a difference in**  
 819 **the 2090 – 2100 decadal means of simulations with and without LUC. The negative values indicate less sink / larger**  
 820 **source from land to atmosphere. (c) The bioenergy crop area in 2100 from LUH2. Latitudinal distributions of the land**  
 821  **$\beta$  and  $\gamma$  feedback parameters (a) globally and (b) in crop-concentrated areas in the SSP5 3.4 OS pathway by five CMIP6**  
 822 **ESMs used in this study. Parameters in crop-concentrated areas are calculated as means of values in the range of**  
 823 **cropland thresholds defined in Text A1.**

824

Mis en forme : Légende

Mis en forme : Vérifier l'orthographe et la grammaire



825

826  
827  
828

**Figure 6: The variation of (a) global  $\beta_{\text{land}}$  ( $\text{GtC ppm}^{-1}$ ) and  $\gamma_{\text{land}}$  ( $\text{GtC } ^\circ\text{C}^{-1}$ ), and (b) cumulative over 2000–2300 (for IPSL-CM6A-LR) and over 2000–2100 (for MIROC-ES2L)  $\beta$ - and  $\gamma$ -driven land carbon uptakes with and without LUC. The changes in LUC are given as 9-year moving averages, negative value corresponds to a land sink.**

- Mis en forme : Indice
- Mis en forme : Légende
- Mis en forme : Expositant
- Mis en forme : Indice
- Mis en forme : Expositant